

# Quantum Algorithm for Dynamic Mode Decomposition and Matrix Eigenvalue Decomposition with Complex Eigenvalues

Yuta Mizuno<sup>1,2,3,\*</sup> and Tamiki Komatsuzaki<sup>1,2,3,4</sup>

<sup>1</sup>*Research Institute for Electronic Science, Hokkaido University, Sapporo, Hokkaido 001-0020, Japan*

<sup>2</sup>*Institute for Chemical Reaction Design and Discovery (WPI-ICReDD),  
Hokkaido University, Sapporo, Hokkaido 001-0021, Japan*

<sup>3</sup>*Graduate School of Chemical Sciences and Engineering,  
Hokkaido University, Sapporo, Hokkaido 060-8628, Japan*

<sup>4</sup>*The Institute of Scientific and Industrial Research,  
Osaka University, Ibaraki, Osaka 567-0047, Japan*

(Dated: December 4, 2023)

We present a quantum algorithm that analyzes time series data simulated by a quantum differential equation solver. The proposed algorithm is a quantum version of the dynamic mode decomposition algorithm used in diverse fields such as fluid dynamics and epidemiology. Our quantum algorithm can also extract matrix eigenvalues by analyzing the corresponding linear dynamical system. Our algorithm handles a broader range of matrices with complex eigenvalues, unlike existing efficient quantum eigensolvers limited to specific matrix types. The complexity of our quantum algorithm is  $O(\text{poly log } N)$  for an  $N$ -dimensional system. This is an exponential speedup over known classical algorithms with at least  $O(N)$  complexity. Thus, our quantum algorithm is expected to enable high-dimensional dynamical systems analysis and large matrix eigenvalue decomposition, intractable for classical computers.

## I. INTRODUCTION

Quantum algorithms provide exponential speedup over classical algorithms for numerical linear algebra tasks such as eigenvalue decomposition of unitary or Hermitian matrices [1–3], singular value decomposition of low-rank matrices [4, 5], and solving linear systems of equations [6, 7]. These quantum algorithms can solve problems of  $N$  dimensions in runtime  $O(\text{poly log } N)$ . They have significant applications in quantum chemistry [8], machine learning [4, 9], and solving differential equations [10–13].

Quantum numerical linear algebra also offers prospects for advancements in dynamical systems analysis. A probability density function on the state space of a dynamical system is advanced in time by the Perron–Frobenius operator [14, 15]. Meanwhile, the Koopman operator is responsible for the time evolution of observable functions on the state space [14, 15]. These operators are linear operators on infinite-dimensional function spaces. In other words, any finite-dimensional (possibly nonlinear) dynamical system can be described as an infinite-dimensional linear dynamical system. Therefore, linear algebraic techniques such as spectral decomposition can be applied to general dynamical systems analysis.

To numerically analyze such an infinite-dimensional linear system, one may resort to a finite-dimensional approximation. This often leads to a linear system with an extremely-large number of dimensions  $N(\gg 1)$ . Such high-dimensional systems may be simulated using a quantum linear differential equation solver (QLDES) [10–12] in runtime  $O(\text{poly log } N)$ . The quantum solver yields

a quantum state whose amplitudes encode time series data of the dynamical system. However, as the tomography of such quantum state takes a runtime of  $O(N)$ , an efficient method for extracting essential, dynamical information from the quantum data is highly demanded.

We propose a novel quantum algorithm for dynamic mode decomposition (DMD), a numerical technique that estimates the spectral decomposition of the Koopman operator of a dynamical system from its time-series data [14]. This spectral decomposition elucidates the essential temporal behavior of the dynamical system. Classical DMD algorithms are frequently applied in various fields such as fluid dynamics and epidemiology [14].

Quantum algorithms for the spectral estimation from time-series data have been proposed by Steffens et al. [16] and Xue et al. [17]; however, these algorithms presuppose time-series data stored in a quantum random access memory or specific amplitude encoding, and efficiently preparing such data with a QLDES remains a challenge. Furthermore, this disconnection between simulation and time-series analysis on a quantum computer can be potentially an obstacle to exponential speedup achieved by each part. In contrast, our quantum DMD (qDMD) algorithm proposed in this article offers an implementable and seamless protocol to analyze QLDES-generated time-series data on a quantum computer. Consequently, our algorithm fills the critical gap in simulation and data analysis, achieving an exponential speedup over classical algorithms with respect to the system’s dimension  $N$ .

Our qDMD algorithm can also serve as a quantum subroutine for eigenvalue decomposition of matrices, especially those with complex eigenvalues. If a linear differential equation  $\dot{\mathbf{x}} = \mathbf{A}\mathbf{x}$  can be simulated efficiently on a quantum computer, our algorithm can efficiently compute approximate eigenvalues and eigenvectors of

---

\* mizuno@es.hokudai.ac.jp

$\exp(\Delta t \mathbf{A})$ , where  $\Delta t$  is the time step of the simulation. Notably, the matrix  $\mathbf{A}$  is not restricted to Hermitian and may have complex eigenvalues. Therefore, the composite protocol of a QLDES and our qDMD algorithm can be considered as a generalization of quantum phase estimation [1–3], which combines Hamiltonian dynamics simulation and quantum Fourier transform. Although previous studies [18–21] have pioneered quantum eigensolvers for complex eigenvalue problems, these approaches have limitations such as the lack of the theoretical guarantee of an exponential speedup and requiring a specific form of input states. Our qDMD algorithm is designed to be free from such limitations.

## II. DYNAMIC MODE DECOMPOSITION

We introduce the *exact DMD* algorithm proposed by Tu et al. [22]. Let us consider an  $N$ -dimensional linear dynamical system  $\dot{\mathbf{x}} = \mathbf{A}\mathbf{x}$ , where  $\mathbf{x} \in \mathbb{C}^N$ , and  $\mathbf{A} \in \mathbb{C}^{N \times N}$  is a diagonalizable matrix<sup>1</sup>. Let  $\mathbf{K}$  denote the time evolution operator with time step  $\Delta t$ :  $\mathbf{K} := \exp(\Delta t \mathbf{A})$ . Suppose we have a collection of  $M$  snapshot pairs of time-series data, symbolized as  $\{(\mathbf{x}_j, \mathbf{x}'_j)\}_{j=0}^{M-1}$ . Here  $\mathbf{x}'_j$  signifies the state observed at the subsequent time step following  $\mathbf{x}_j$ :  $\mathbf{x}'_j \approx \mathbf{K}\mathbf{x}_j$ <sup>2</sup>. Note that  $\mathbf{x}_j$ 's can be taken from multiple different trajectories. From the data, we can estimate the time-evolution operator  $\mathbf{K}$  as

$$\tilde{\mathbf{K}} = \operatorname{argmin}_{\mathbf{K} \in \mathbb{C}^{N \times N}} \|\mathbf{X}' - \mathbf{K}\mathbf{X}\|_{\text{F}} = \mathbf{X}'\mathbf{X}^+, \quad (1)$$

where  $\tilde{\mathbf{K}}$  signifies the approximation of the underlying  $\mathbf{K}$ ,  $\|\cdot\|_{\text{F}}$  denotes the Frobenius norm,  $\mathbf{X} := [\mathbf{x}_0 \cdots \mathbf{x}_{M-1}]$ ,  $\mathbf{X}' := [\mathbf{x}'_0 \cdots \mathbf{x}'_{M-1}]$ , and  $\mathbf{X}^+$  is the pseudo-inverse of  $\mathbf{X}$ . The construction of  $N \times N$  matrix  $\tilde{\mathbf{K}}$  and its eigenvalue decomposition becomes intractable as  $N$  increases. Thus, we solve the eigenvalue problem of the following projected matrix instead:

$$\tilde{\mathbf{K}}' = \mathbf{Q}^\dagger \tilde{\mathbf{K}} \mathbf{Q}, \quad (2)$$

where  $\mathbf{Q}$  is an  $N \times R$  matrix whose columns are the  $R$  dominant left singular vectors of the  $N \times 2M$  matrix  $[\mathbf{X} \ \mathbf{X}']$ . The effective rank  $R$  is determined so that the error of the rank- $R$  approximation of  $[\mathbf{X} \ \mathbf{X}']$  in the Frobenius norm is less than a specified tolerance. The exact DMD algorithm assumes that  $R$  is sufficiently smaller than  $N$  so that the eigenvalue decomposition of the  $R \times R$  matrix  $\tilde{\mathbf{K}}'$  can be computed practically on a classical computer. The eigenvalue decomposition of  $\tilde{\mathbf{K}}'$  approximates that of  $\tilde{\mathbf{K}}$  as

$$\tilde{\lambda}_r \approx \tilde{\lambda}'_r, \quad \tilde{\mathbf{w}}_r \approx \mathbf{Q}\tilde{\mathbf{w}}'_r \quad (r = 1, \dots, R). \quad (3)$$

Here,  $\tilde{\lambda}_r$  and  $\tilde{\mathbf{w}}_r$  (resp.  $\tilde{\lambda}'_r$  and  $\tilde{\mathbf{w}}'_r$ ) are the  $r$ -th eigenvalue and eigenvector of  $\tilde{\mathbf{K}}$  (resp.  $\tilde{\mathbf{K}}'$ ). The real part and the imaginary part of  $(\ln \tilde{\lambda}_r)/\Delta t$  correspond to the decay/growth rate and the oscillation frequency of the  $r$ -th DMD mode, respectively. The computational complexity of this algorithm is  $O(\min(NM^2, MN^2))$  for the singular value decomposition (SVD) and  $O(R^3)$  for the eigenvalue decomposition of  $\tilde{\mathbf{K}}'$  [23].

## III. qDMD ALGORITHM

Our qDMD algorithm consists of the following five steps:

1. Prepare quantum states encoding  $\mathbf{X}$  and  $\mathbf{X}'$  using a QLDES.
2. Compute the SVDs of  $\mathbf{X}$ ,  $\mathbf{X}'$ , and  $[\mathbf{X} \ \mathbf{X}']$  on a quantum computer.
3. Estimate the elements of  $\tilde{\mathbf{K}}'$  from the quantum data and construct  $\tilde{\mathbf{K}}'$  as classical data.
4. Solve the eigenvalue problem of  $\tilde{\mathbf{K}}'$  on a classical computer.
5. Compute a quantum state encoding  $\tilde{\mathbf{w}}_r$ .

Steps 1–3, and 5 are efficiently executed on a quantum computer in runtime  $O(\text{poly log } N)$  as shown below. Given that  $R \ll N$ , step 4 can be handled by a classical computer. Consequently, our qDMD algorithm is exponentially faster than its classical counterpart with respect to  $N$ . Similar quantum-classical hybrid strategies are also employed by Steffens et al. [16] and Xue et al. [17], though the specifics of the quantum procedures differ.

In what follows, we will expound the quantum procedures of steps 1–3 and 5. Henceforth, we adopt the following notation: The computational basis whose bit string represents integer  $i$  is denoted by  $|i\rangle$ . As necessary, we denote a ket vector of the  $k$ -th quantum register like  $|\rangle_k$ . For vector  $\mathbf{v} = (v^0, \dots, v^{n-1})^\top \in \mathbb{C}^n$ , we define  $|\mathbf{v}\rangle := \sum_{i=0}^{n-1} v^i |i\rangle$ . Similarly, for matrix  $\mathbf{Z} = [\mathbf{v}_0 \cdots \mathbf{v}_{m-1}] \in \mathbb{C}^{n \times m}$ , we write  $|\mathbf{Z}\rangle := \sum_{j=0}^{m-1} |\mathbf{v}_j\rangle |j\rangle = \sum_{i=0}^{n-1} \sum_{j=0}^{m-1} v_j^i |i\rangle |j\rangle$ . A normalized matrix  $\mathbf{Z}/\|\mathbf{Z}\|_{\text{F}}$  is denoted by  $\hat{\mathbf{Z}}$ , thus  $|\hat{\mathbf{Z}}\rangle$  symbolizes the normalized ket vector (quantum state) proportional to  $|\mathbf{Z}\rangle$ . Additionally, the  $r$ -th singular value, left and right singular vectors of matrix  $\mathbf{Z}$  are designated by  $\sigma_r^{\mathbf{Z}}$ ,  $\mathbf{u}_r^{\mathbf{Z}}$ , and  $\mathbf{v}_r^{\mathbf{Z}}$ , respectively. The notation of quantum circuit diagrams we employ can be found in [24].

### A. Step 1

The quantum circuit shown in Fig. 1 is responsible for preparing the quantum state encoding  $\mathbf{X}$  and  $\mathbf{X}'$ . Here, we prepare time-series data of  $L$  different trajectories of  $(T+1)$  time steps. Consequently, the number of columns  $M$  equals  $(T+1)L$  in this article.

<sup>1</sup> For the case that  $A$  is not diagonalizable, see discussion in Supplemental Material.

<sup>2</sup> Since numerical integration of a linear differential equation involves approximations, the simulated data  $\mathbf{x}'_j$  is an approximation of the exact solution  $\mathbf{K}\mathbf{x}_j$

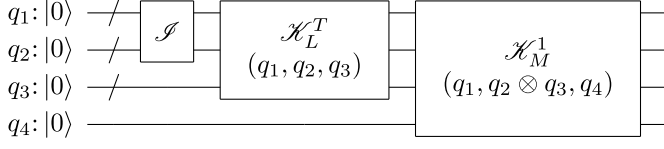


FIG. 1. Quantum circuit for data matrix preparation.  $\mathcal{S}$  is a quantum oracle for initial state preparation.  $\mathcal{K}_\mu^\tau$  is a quantum algorithm that simulates the dynamics up to the  $\tau$ -th time step for  $\mu$  initial conditions. The label of each of the simulation gate indicates which registers the gate acts on; e.g. label  $(q_i, q_k, q_t)$  indicates that the simulation gate is performed on the registers  $q_i$ ,  $q_k$ , and  $q_t$ , which correspond to the first, second, and third registers in Eq. 5, respectively.

We assume a quantum oracle  $\mathcal{S}$  that generates a superposition of  $L$  initial states  $\{\mathbf{x}_k\}_{k=0}^{L-1}$  as

$$|0\rangle|0\rangle \xrightarrow{\mathcal{S}} \sum_{k=0}^{L-1} |\mathbf{x}_k\rangle|k\rangle. \quad (4)$$

Here, the normalizing constant for the right hand side is omitted. We also introduce a quantum subroutine  $\mathcal{K}_\mu^\tau$  that simulates the linear dynamical system up to the  $\tau$ -th time step for  $\mu$  initial conditions:

$$\sum_{k=0}^{\mu-1} |\mathbf{x}_k\rangle|k\rangle|0\rangle \xrightarrow{\mathcal{K}_\mu^\tau} \sum_{k=0}^{\mu-1} \sum_{t=0}^{\tau} |\tilde{\mathbf{x}}_k(t, \Delta t)\rangle|k\rangle|t\rangle, \quad (5)$$

where  $\tilde{\mathbf{x}}_k(t, \Delta t)$  is the simulated state at the  $t$ -th time step of the trajectory initiated from  $\mathbf{x}_k$ , and the normalizing constants for the both sides are omitted. We can implement  $\mathcal{K}_\mu^\tau$  by the Taylor series method and a quantum linear systems solver with gate complexity  $O(\tau \text{ poly}(\log(N\tau\mu/\epsilon)))$  [11, 25], where  $\epsilon$  denotes the tolerance for simulation error.

Applying  $\mathcal{S}$  and  $\mathcal{K}_L^T$  to registers  $q_1$ ,  $q_2$ , and  $q_3$ , we get

$$|\mathbf{X}\rangle = \sum_{k=0}^{L-1} \sum_{t=0}^T |\tilde{\mathbf{x}}_k(t, \Delta t)\rangle_1 |t + (T+1)k\rangle_{23}. \quad (6)$$

In this context, the register  $q_1$  encodes states of the dynamical system, and the registers  $q_2$  and  $q_3$ —indicating the initial condition  $k$  and the time step count  $t$ —collectively label the column index of  $\mathbf{X}$  as  $|t + (T+1)k\rangle_{23} = |k\rangle_2 |t\rangle_3$ . Regarding the  $M$  columns of  $\mathbf{X}$  as initial states and the register  $q_4$  as the time step counter, the one-step simulation gate  $\mathcal{K}_M^1$  generates the quantum state proportional to

$$|[\mathbf{X} \ \mathbf{X}']\rangle = |\mathbf{X}\rangle|0\rangle_4 + |\mathbf{X}'\rangle|1\rangle_4. \quad (7)$$

This ket vector can be viewed as encoding  $[\mathbf{X} \ \mathbf{X}']$ , regarding  $q_2 \otimes q_3 \otimes q_4$  as indicating the column index collectively. Measuring the fourth register, we obtain a quantum state  $|\hat{\mathbf{X}}\rangle$  or  $|\hat{\mathbf{X}}'\rangle$ .

## B. Step 2

According to the procedure proposed by Schuld et al. [9], we perform the SVD of a normalized matrix  $\hat{\mathbf{Z}}$  ( $\mathbf{Z} = \mathbf{X}, \mathbf{X}'$ , or  $[\mathbf{X} \ \mathbf{X}']$ ) on a quantum computer using  $C$  copies of  $|\hat{\mathbf{Z}}\rangle$  as

$$|\hat{\mathbf{Z}}\rangle^{\otimes C} \mapsto |\text{SVD}(\hat{\mathbf{Z}})\rangle \approx \sum_{r=1}^R \hat{\sigma}_r^{\mathbf{Z}} |\mathbf{u}_r^{\mathbf{Z}}\rangle |\mathbf{v}_r^{\mathbf{Z}*}\rangle |(\hat{\sigma}_r^{\mathbf{Z}})^2\rangle_5, \quad (8)$$

where  $\hat{\sigma}_r^{\mathbf{Z}} := \sigma_r^{\mathbf{Z}} = \sigma_r^{\mathbf{Z}} / \|\mathbf{Z}\|_{\text{F}}$ , and  $|(\hat{\sigma}_r^{\mathbf{Z}})^2\rangle_5$  designates the computational basis of the extra fifth register indicating the binary representation of  $(\hat{\sigma}_r^{\mathbf{Z}})^2$ . Note that matrix normalization does not change singular vectors:  $\mathbf{u}_r^{\hat{\mathbf{Z}}} = \mathbf{u}_r^{\mathbf{Z}}$  and  $\mathbf{v}_r^{\hat{\mathbf{Z}}} = \mathbf{v}_r^{\mathbf{Z}}$ . Thus we omit the hat ( $\hat{\cdot}$ ) in the superscript of singular vectors for brevity. This quantum SVD process utilizes density matrix exponentiation [4] and quantum phase estimation. The necessary number of state copies  $C$  for precision  $\epsilon$  is  $O(1/\epsilon^2)$  [26].

## C. Step 3

The estimation of  $\tilde{\mathbf{K}}'$  is based on the following factorization:

$$\tilde{\mathbf{K}}' \approx \frac{\|\mathbf{X}'\|_{\text{F}}}{\|\mathbf{X}\|_{\text{F}}} (\mathbf{Q}^\dagger \mathbf{U}') \hat{\Sigma}' (\mathbf{V}'^\dagger \mathbf{V}) \hat{\Sigma}^{-1} (\mathbf{U}^\dagger \mathbf{Q}), \quad (9)$$

where  $\hat{\mathbf{X}} \approx \mathbf{U} \hat{\Sigma} \mathbf{V}^\dagger$  and  $\hat{\mathbf{X}}' \approx \mathbf{U}' \hat{\Sigma}' \mathbf{V}'^\dagger$  are the SVDs of the normalized data matrices with rank- $R$  truncation. The first factor  $\|\mathbf{X}'\|_{\text{F}} / \|\mathbf{X}\|_{\text{F}}$  ( $= \|\mathbf{X}'\| / \|\mathbf{X}\|$ ) can be estimated by measuring the fourth register of  $[[\mathbf{X} \ \mathbf{X}']\rangle$  because the probability ratio of measured values 1 to 0,  $\Pr(q_4 = 1) / \Pr(q_4 = 0)$ , equals the square of this factor. The diagonal elements of  $\hat{\Sigma}$  and  $\hat{\Sigma}'$ , i.e.,  $\{\hat{\sigma}_r^{\mathbf{X}}\}_{r=1}^R$  and  $\{\hat{\sigma}_r^{\mathbf{X}'}\}_{r=1}^R$ , can be estimated by measuring the fifth register of  $|\text{SVD}(\hat{\mathbf{X}})\rangle$  and  $|\text{SVD}(\hat{\mathbf{X}}')\rangle$ . All the off-diagonal elements of  $\hat{\Sigma}$  and  $\hat{\Sigma}'$  are zero. The elements of matrices  $\mathbf{Q}^\dagger \mathbf{U}'$ ,  $\mathbf{U}^\dagger \mathbf{Q}$ , and  $\mathbf{V}'^\dagger \mathbf{V}$  are inner products between singular vectors. Note that the  $r$ -th column vector of  $\mathbf{Q}$  corresponds to  $\mathbf{u}_r^{[\mathbf{X} \ \mathbf{X}']}$ . Now, the remaining task is to estimate  $\langle \mathbf{u}_r^{[\mathbf{X} \ \mathbf{X}']} | \mathbf{u}_{r'}^{\mathbf{X}'} \rangle$ ,  $\langle \mathbf{u}_r^{\mathbf{X}} | \mathbf{u}_{r'}^{[\mathbf{X} \ \mathbf{X}']} \rangle$ , and  $\langle \mathbf{v}_r^{\mathbf{X}'} | \mathbf{v}_{r'}^{\mathbf{X}} \rangle$  for  $R^2$  combinations of  $r$  and  $r'$ .

The two-state SWAP test depicted in Fig. 2 (a) is often employed for estimating the absolute value of the inner product between arbitrary quantum states  $|\psi_0\rangle$  and  $|\psi_1\rangle$ . However, the two-state SWAP test cannot estimate the phase (argument) of the inner product. Furthermore, the global phase of a singular vector is arbitrary. For instance, if we have a singular vector pair  $(|\mathbf{u}_r\rangle, |\mathbf{v}_r^*\rangle)$ , then  $(e^{i\theta}|\mathbf{u}_r\rangle, e^{-i\theta}|\mathbf{v}_r^*\rangle)$  is also a valid pair, where  $\theta$  ranges from 0 to  $2\pi$ . The choice of the global phase of the singular vector pair changes inner products to be estimated. To overcome these challenges, we introduce the *three-state SWAP test* (Fig. 2 (b)) and *reference states* for the left and right singular vectors.

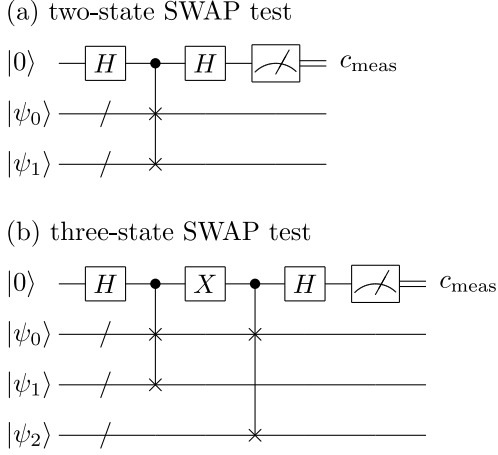


FIG. 2. Quantum circuit for inner product estimation using controlled SWAP gates. The input states  $|\psi_k\rangle$  ( $k = 0, 1, 2$ ) are arbitrary quantum states. (a) In the two-state SWAP test,  $\Pr[c_{\text{meas}} = 0] - \Pr[c_{\text{meas}} = 1] = |\langle\psi_0|\psi_1\rangle|^2$ . (b) In the three-state SWAP test,  $\Pr[c_{\text{meas}} = 0] - \Pr[c_{\text{meas}} = 1] = \text{Re}(\langle\psi_0|\psi_1\rangle\langle\psi_1|\psi_2\rangle\langle\psi_2|\psi_0\rangle)$ . When the phase gate  $S^\dagger$  is inserted after the first Hadamard gate,  $\Pr[c_{\text{meas}} = 0] - \Pr[c_{\text{meas}} = 1] = \text{Im}(\langle\psi_0|\psi_1\rangle\langle\psi_1|\psi_2\rangle\langle\psi_2|\psi_0\rangle)$ .

First, we estimate the inner products between left sin-

$$\frac{1}{\sqrt{2}\|\mathbf{X} \mathbf{X}'\|_F} \left[ \|\mathbf{X}\|_F \sum_{r=1}^R \hat{\sigma}_r^{\mathbf{X}} |\mathbf{u}_r^{\mathbf{X}}\rangle_1 |\mathbf{v}_r^{\mathbf{X}*}\rangle_{23} |0\rangle_4 |(\hat{\sigma}_r^{\mathbf{X}})^2\rangle_5 + |\mathbf{X}'\rangle_{123} |1\rangle_4 |0\rangle_5 \right] |0\rangle_6 + \frac{1}{\sqrt{2}} |\chi_1\rangle_1 |\chi_2\rangle_{23} |0\rangle_4 |0\rangle_5 |1\rangle_6. \quad (10)$$

Next, we input this state to the circuit shown in Fig. 4. The upper quantum register of the circuit corresponds to  $q_1 \otimes q_2 \otimes q_3$  and the bottom corresponds to  $q_4 \otimes q_5 \otimes q_6$ . Let us set  $|0\rangle_4 |0\rangle_5 |1\rangle_6$  and  $|0\rangle_4 |(\hat{\sigma}_r^{\mathbf{X}})^2\rangle_5 |0\rangle_6$  to  $|i\rangle$  and  $|j\rangle$  in the circuit diagram. Then, the circuit provides an estimate of  $\langle\chi_1|\mathbf{u}_r^{\mathbf{X}}\rangle\langle\chi_2|\mathbf{v}_r^{\mathbf{X}*}\rangle$ . Since we know the value of  $\langle\chi_1|\mathbf{u}_r^{\mathbf{X}}\rangle$ , we can derive an estimate of  $\langle\chi_2|\mathbf{v}_r^{\mathbf{X}*}\rangle$ . Likewise, we can estimate  $\langle\chi_2|\mathbf{v}_r^{\mathbf{X}*}\rangle$  with applying the Step2 gate conditionally on  $q_4 = 1$  in the circuit of Fig. 3.

The number of quantum SVDs necessary for estimating  $\tilde{\mathbf{K}}'$  with precision  $\epsilon$  is  $O(1/\epsilon^2 \text{ poly } R)$ , excluding reference state preparation costs. The factor  $O(1/\epsilon^2)$  originates from sampling errors obeying the central limit theorem. While preparing the reference states may require additional  $O(M)$  quantum SVDs, the overall gate complexity remains at  $O(\text{poly log } N)$ . A detailed discussion

of the computational complexity can be found in Supplemental Material.

regular vectors. We define the global phase of each left singular vector state  $|\mathbf{u}\rangle$  such that  $\arg\langle\chi_1|\mathbf{u}\rangle = 0$  for a fixed reference quantum state  $|\chi_1\rangle$ <sup>3</sup>. The two-state SWAP test between  $|\chi_1\rangle$  and  $|\mathbf{u}\rangle$  estimates  $|\langle\chi_1|\mathbf{u}\rangle|$ . Here, the singular vector state  $|\mathbf{u}\rangle$  can be prepared by executing the quantum SVD and measuring the fifth register encoding squared singular values. Additionally, the three-state SWAP test between  $|\chi_1\rangle$  and arbitrary left singular vector states  $|\mathbf{u}\rangle$  and  $|\mathbf{u}'\rangle$  provides an estimate of  $\langle\chi_1|\mathbf{u}\rangle\langle\mathbf{u}|\mathbf{u}'\rangle\langle\mathbf{u}'|\chi_1\rangle$ . Leveraging the known absolute values and phases of  $\langle\chi_1|\mathbf{u}\rangle$  and  $\langle\mathbf{u}'|\chi_1\rangle$ , we can derive an estimate of  $\langle\mathbf{u}|\mathbf{u}'\rangle$ . In this way,  $\langle\mathbf{u}_r^{\mathbf{X}}|\mathbf{u}_{r'}^{\mathbf{X}}\rangle$  and  $\langle\mathbf{u}_r^{\mathbf{X}}|\mathbf{u}_{r'}^{\mathbf{X}'}\rangle$  can be estimated.

Next, we estimate the inner products between right singular vectors. Since the global phase of a right singular vector is synchronized with that of the associated left singular vector, we cannot arbitrarily define  $\arg\langle\chi_2|\mathbf{v}^*\rangle$  for a fixed reference state  $|\chi_2\rangle$ <sup>3</sup> and a right singular vector state  $|\mathbf{v}^*\rangle$ ; instead, we also need to estimate  $\arg\langle\chi_2|\mathbf{v}^*\rangle$ . Once we determine  $\langle\chi_2|\mathbf{v}^*\rangle$  for every right singular vector  $\mathbf{v}$ , we can estimate  $\langle\mathbf{v}_r^{\mathbf{X}'}|\mathbf{v}_{r'}^{\mathbf{X}'}\rangle$  using the three-state SWAP test as described above. Thus, let us consider how to determine  $\langle\chi_2|\mathbf{v}^*\rangle$ . First, we prepare the following quantum state using the quantum circuit depicted in Fig. 3 with applying the Step2 gate conditionally on  $q_4 = 0$ :

of the computational complexity can be found in Supplemental Material.

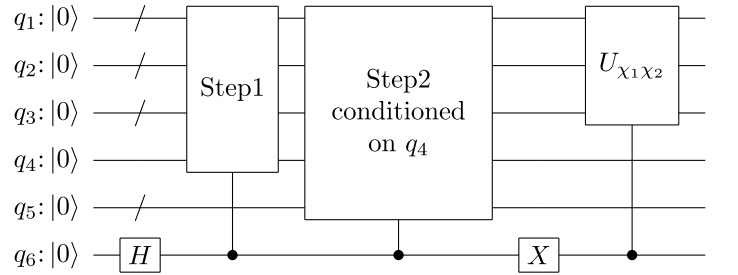


FIG. 3. Quantum circuit for generating input states for the circuit of Fig. 4. The Step1 gate generates  $|\mathbf{X} \hat{\mathbf{X}}'\rangle$ , corresponding to the circuit in Fig. 1. The Step2 gate performs the quantum SVD conditionally on the register  $q_4$ . When applied conditionally on  $q_4 = 0$  (resp.  $q_4 = 1$ ), this gate performs the quantum SVD of  $\hat{\mathbf{X}}$  (resp.  $\hat{\mathbf{X}}'$ ). The unitary gate  $U_{\chi_1 \chi_2}$  creates the reference states as  $U_{\chi_1 \chi_2} |0\rangle_1 |0\rangle_{23} = |\chi_1\rangle_1 |\chi_2\rangle_{23}$ .

<sup>3</sup> The reference states,  $|\chi_1\rangle$  and  $|\chi_2\rangle$ , can be chosen arbitrarily, provided that  $\langle\chi_1|\mathbf{u}\rangle \neq 0$  and  $\langle\chi_2|\mathbf{v}^*\rangle \neq 0$  for all left and right singular vectors  $\mathbf{u}$  and  $\mathbf{v}$ . However, the choice of  $|\chi_1\rangle$  and  $|\chi_2\rangle$  affects the algorithm's efficiency (see Supplemental Material).

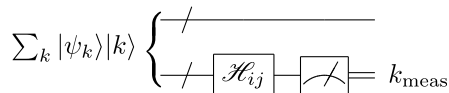


FIG. 4. Quantum circuit for inner product estimation using a Hadamard gate. Gate  $\mathcal{H}_{ij}$  is defined by  $H_{ij} + I_{ij}^\perp$ . Here,  $H_{ij}$  is the Hadamard gate on the 2-dimensional Hilbert space  $\mathcal{H} := \text{span}\{|i\rangle, |j\rangle\}$ , i.e.,  $H_{ij} := (|i\rangle\langle i| + |i\rangle\langle j| + |j\rangle\langle i| - |j\rangle\langle j|)/\sqrt{2}$ , and  $I_{ij}^\perp$  is the identity operator on the orthogonal complementary space of  $\mathcal{H}$ . The  $|\psi_k\rangle$ 's are arbitrary unnormalized ket vectors. The measurement probability satisfies  $\text{Pr}[k_{\text{meas}} = i] - \text{Pr}[k_{\text{meas}} = j] = 2 \text{Re} \langle \psi_i | \psi_j \rangle$ . When the phase shift  $|j\rangle \mapsto -i|j\rangle$  is applied before  $\mathcal{H}_{ij}$ ,  $\text{Pr}[k_{\text{meas}} = i] - \text{Pr}[k_{\text{meas}} = j] = 2 \text{Im} \langle \psi_i | \psi_j \rangle$ .

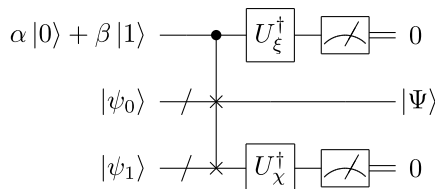


FIG. 5. Quantum circuit for coherent addition of two quantum states  $|\psi_0\rangle$  and  $|\psi_1\rangle$  [27].  $U_\chi$  is a unitary gate satisfying  $U_\chi |0\rangle = |\chi\rangle$ .  $U_\xi$  is a unitary gate satisfying  $U_\xi |0\rangle = |\xi\rangle$ , where  $|\xi\rangle := \sqrt{c_0/(c_0 + c_1)}|0\rangle + \sqrt{c_1/(c_0 + c_1)}|1\rangle$ . If the measured values of the first and third registers are both zero, the coherent addition has been successful.

#### D. Step 5

A quantum state encoding the  $r$ -th DMD mode is given by

$$|\tilde{\mathbf{w}}_r\rangle \approx \sum_{r'=1}^R \tilde{w}_r^{r'} |\mathbf{u}_{r'}^{[\mathbf{x}, \mathbf{x}']}\rangle, \quad (11)$$

where  $\tilde{\mathbf{w}}_r = (\tilde{w}_r^{1}, \dots, \tilde{w}_r^{R})^\top$  is computed at step 4. Such coherent superposition of quantum states can be created using the quantum circuit shown in Fig. 5. This circuit creates a superposition of  $|\psi_0\rangle$  and  $|\psi_1\rangle$  [27]:

$$|\Psi\rangle = \alpha \frac{\langle \chi | \psi_1 \rangle}{|\langle \chi | \psi_1 \rangle|} |\psi_0\rangle + \beta \frac{\langle \chi | \psi_0 \rangle}{|\langle \chi | \psi_0 \rangle|} |\psi_1\rangle. \quad (12)$$

Here,  $\alpha$  and  $\beta$  are user-specified complex amplitudes, and  $|\chi\rangle$  is a reference quantum state. This addition process is probabilistic. The success probability is  $c_0 c_1 / (c_0 + c_1)$  if  $\langle \psi_0 | \psi_1 \rangle = 0$ , where  $c_i = |\langle \chi | \psi_i \rangle|^2$ . By recursively creating coherent superpositions of two states, we can construct the multi-state superposition  $|\tilde{\mathbf{w}}_r\rangle$  with  $O(\text{poly } R)$  times of the quantum SVD (see Supplemental Material).

## IV. CONCLUSION

The qDMD algorithm performs DMD on quantum time series data generated by a QLDES. This algorithm is also capable of computing (possibly complex) eigenvalues and eigenvectors of matrices. Excluding reference state preparation costs, the total gate complexity scales as  $O(T \text{ poly log}(NM/\epsilon) \text{ poly}(R)/\epsilon^4)$ . The qDMD algorithm can achieve an exponential speedup over its classical counterpart in terms of  $N$  if  $R$  remains at most  $O(\text{poly log } N)$ . Since the algorithm utilizes density matrix exponentiation and sampling-based inner product estimation, the dependency on  $\epsilon$  is less optimal than that of the classical counterpart. Reducing the complexity with respect to  $\epsilon$  should be addressed in future work.

## ACKNOWLEDGMENTS

This work was supported by JST, PRESTO Grant Number JPMJPR2018, Japan, and partially by Crossover Alliance to Create the Future with People, Intelligence and Materials, Japan (to YM).

- 
- [1] A. Y. Kitaev, Quantum measurements and the abelian stabilizer problem (1995), arXiv:quant-ph/9511026 [quant-ph].
  - [2] R. Cleve, A. Ekert, C. Macchiavello, and M. Mosca, Quantum algorithms revisited, Proceedings of the Royal Society of London. Series A: Mathematical, Physical and Engineering Sciences **454**, 339 (1998).
  - [3] D. S. Abrams and S. Lloyd, Quantum algorithm providing exponential speed increase for finding eigenvalues and eigenvectors, Physical Review Letters **83**, 5162 (1999).
  - [4] S. Lloyd, M. Mohseni, and P. Rebentrost, Quantum principal component analysis, Nature Physics **10**, 631 (2014).
  - [5] P. Rebentrost, A. Steffens, I. Marvian, and S. Lloyd, Quantum singular-value decomposition of nonsparse low-rank matrices, Physical Review A **97**, 012327 (2018).
  - [6] A. W. Harrow, A. Hassidim, and S. Lloyd, Quantum algorithm for linear systems of equations, Physical Review Letters **103**, 150502 (2009).
  - [7] A. M. Childs, R. Kothari, and R. D. Somma, Quantum algorithm for systems of linear equations with exponentially improved dependence on precision, SIAM Journal on Computing **46**, 1920 (2017).
  - [8] A. Aspuru-Guzik, A. D. Dutoi, P. J. Love, and M. Head-Gordon, Simulated quantum computation of molecular energies, Science **309**, 1704 (2005).
  - [9] M. Schuld, I. Sinayskiy, and F. Petruccione, Prediction by linear regression on a quantum computer, Physical Review A **94**, 022342 (2016).
  - [10] D. W. Berry, High-order quantum algorithm for solving linear differential equations, Journal of Physics A: Mathematical and Theoretical **47**, 105301 (2014).

- [11] D. W. Berry, A. M. Childs, A. Ostrander, and G. Wang, Quantum algorithm for linear differential equations with exponentially improved dependence on precision, *Communications in Mathematical Physics* **356**, 1057 (2017).
- [12] A. M. Childs and J.-P. Liu, Quantum spectral methods for differential equations, *Communications in Mathematical Physics* **375**, 1427 (2020).
- [13] J.-P. Liu, H. Ø. Kolden, H. K. Krovi, N. F. Loureiro, K. Trivisa, and A. M. Childs, Efficient quantum algorithm for dissipative nonlinear differential equations, *Proceedings of the National Academy of Sciences* **118**, e2026805118 (2021).
- [14] S. L. Brunton, M. Budišić, E. Kaiser, and J. N. Kutz, Modern koopman theory for dynamical systems, *SIAM Review* **64**, 229 (2022).
- [15] Y. T. Lin, R. B. Lowrie, D. Aslangil, Y. Subaşı, and A. T. Sornborger, Koopman von neumann mechanics and the koopman representation: A perspective on solving nonlinear dynamical systems with quantum computers (2022), arXiv:2202.02188 [quant-ph].
- [16] A. Steffens, P. Rebentrost, I. Marvian, J. Eisert, and S. Lloyd, An efficient quantum algorithm for spectral estimation, *New Journal of Physics* **19**, 033005 (2017).
- [17] C. Xue, Z.-Y. Chen, T.-P. Sun, X.-F. Xu, S.-M. Chen, H.-Y. Liu, X.-N. Zhuang, Y.-C. Wu, and G.-P. Guo, Quantum dynamic mode decomposition algorithm for high-dimensional time series analysis, *Intelligent Computing* **2**, 0045 (2023).
- [18] H. Wang, L.-A. Wu, Y.-x. Liu, and F. Nori, Measurement-based quantum phase estimation algorithm for finding eigenvalues of non-unitary matrices, *Physical Review A* **82**, 062303 (2010).
- [19] A. Daskin, A. Grama, and S. Kais, A universal quantum circuit scheme for finding complex eigenvalues, *Quantum Information Processing* **13**, 333 (2014).
- [20] A. Teplukhin, B. K. Kendrick, and D. Babikov, Solving complex eigenvalue problems on a quantum annealer with applications to quantum scattering resonances, *Physical Chemistry Chemical Physics* **22**, 26136 (2020).
- [21] C. Shao, Computing eigenvalues of diagonalizable matrices on a quantum computer, *ACM Transactions on Quantum Computing* **3**, 1 (2022).
- [22] J. H. Tu, C. W. Rowley, D. Luchtenburg, S. L. Brunton, and J. N. Kutz, On dynamic mode decomposition: Theory and applications, *Journal of Computational Dynamics* **1**, 391 (2014).
- [23] L. N. Trefethen and D. Bau, *Numerical linear algebra* (Society for Industrial and Applied Mathematics, Philadelphia, United States, 1997).
- [24] M. A. Nielsen and I. L. Chuang, *Quantum Computation and Quantum Information* (Cambridge University Press, Cambridge, United Kingdom, 2010).
- [25] D. Jennings, M. Lostaglio, R. B. Lowrie, S. Pallister, and A. T. Sornborger, The cost of solving linear differential equations on a quantum computer: fast-forwarding to explicit resource counts (2023), arXiv:2309.07881 [quant-ph].
- [26] S. Kimmel, C. Y.-Y. Lin, G. H. Low, M. Ozols, and T. J. Yoder, Hamiltonian simulation with optimal sample complexity, *npj Quantum Information* **3**, 13 (2017).
- [27] M. Oszmaniec, A. Grudka, M. Horodecki, and A. Wójcik, Creating a superposition of unknown quantum states, *Physical Review Letters* **116**, 110403 (2016).

# Supplemental Material for “Quantum Algorithm for Dynamic Mode Decomposition and Matrix Eigenvalue Decomposition with Complex Eigenvalues”

Yuta Mizuno<sup>1,2,3,\*</sup> and Tamiki Komatsuzaki<sup>1,2,3,4</sup>

<sup>1</sup>*Research Institute for Electronic Science, Hokkaido University, Sapporo, Hokkaido 001-0020, Japan*

<sup>2</sup>*Institute for Chemical Reaction Design and Discovery (WPI-ICReDD), Hokkaido University, Sapporo, Hokkaido 001-0021, Japan*

<sup>3</sup>*Graduate School of Chemical Sciences and Engineering, Hokkaido University, Sapporo, Hokkaido 060-8628, Japan*

<sup>4</sup>*The Institute of Scientific and Industrial Research, Osaka University, Ibaraki, Osaka 567-0047, Japan*

(Dated: December 4, 2023)

## CONTENTS

I. Computational Complexity of Estimating $\tilde{\mathbf{K}}'$	1
A. Required number of repetitions of each elemental estimation process	2
B. Required number of quantum SVDs for singular value and vector collection	2
C. Required number of quantum SVDs for estimating $\tilde{\mathbf{K}}'$	3
II. Reference State Preparation for the Inner Product Estimation	5
A. Choice of $ \chi_1\rangle$ and $ \chi_2\rangle$	5
B. Computation of $ \chi_1\rangle$ and $ \chi_2\rangle$	8
C. Summary and concluding remarks	12
III. Computing DMD Mode States	12
A. Recursive coherent state addition	12
B. Computational complexity	13
C. Reference state preparation	15
IV. Dynamic Mode Decomposition for Defective Systems	17
References	18

## I. COMPUTATIONAL COMPLEXITY OF ESTIMATING $\tilde{\mathbf{K}}'$

This section offers a detailed analysis of the computational complexity involved in estimating  $\tilde{\mathbf{K}}'$ . We assume that the required precision of each element of  $\tilde{\mathbf{K}}'$  is  $\epsilon$  in this section. Note that we omit the discussion on the computational complexity of preparing reference states for the inner product estimation, which will be presented in the next section.

In what follows, we first evaluate the required number of repetitions of each elemental estimation process, such as the three-state SWAP test for estimating an inner product. Next, we evaluate the required number of quantum SVDs for collecting singular values and their associated singular vector states necessary for the singular value estimation and the two-state and three-state SWAP tests. Because a single quantum SVD process provides a triple of a singular value and its associated left and right singular vector states at random, we need to take into account this probabilistic nature to estimate the required number of quantum SVDs. To this end, we introduce a general theorem on the necessary number of trials of random selection, proven by Brayton [1]. Finally, we evaluate the total number of quantum SVDs necessary for estimating the whole matrix  $\tilde{\mathbf{K}}'$  as well as its gate complexity.

---

\* mizuno@es.hokudai.ac.jp

TABLE I. Summary of the elemental estimation processes in estimating  $\tilde{\mathbf{K}}'$ .

Estimation Target	Input State(s)	Estimation Method	Required Number of Repetitions
$\frac{\ \mathbf{X}'\ _{\mathbb{F}}}{\ \mathbf{X}\ _{\mathbb{F}}}$	$ [\mathbf{X} \ \mathbf{X}']\rangle_{1:4}$	Measuring the 4th register	$O\left(\frac{1}{\epsilon^2}\right)$
$\hat{\sigma}$	$ \hat{\sigma}^2\rangle$	Measuring the register	1
$\langle\chi_1 \mathbf{u}\rangle$	$ \chi_1\rangle,  \mathbf{u}\rangle$	Two-state SWAP test	$O\left(\frac{1}{\epsilon^2}\right)$
$\langle\mathbf{u} \mathbf{u}'\rangle$	$ \chi_1\rangle,  \mathbf{u}\rangle,  \mathbf{u}'\rangle$	Three-state SWAP test	$O\left(\frac{1}{ \langle\chi_1 \mathbf{u}\rangle ^2 \langle\chi_1 \mathbf{u}'\rangle ^2\epsilon^2}\right)$
$\langle\mathbf{v} \mathbf{v}'\rangle$	$ \chi_2\rangle,  \mathbf{v}^*\rangle,  \mathbf{v}'^*\rangle$	Three-state SWAP test	$O\left(\frac{1}{ \langle\chi_2 \mathbf{v}^*\rangle ^2 \langle\chi_2 \mathbf{v}'^*\rangle ^2\epsilon^2}\right)$
$\langle\chi_2 \mathbf{v}_r^{\mathbf{Z}*}\rangle$	$ 0\rangle_{1:6}$	Circuit shown in Figs. 3 and 4 of the main paper	$O\left(\frac{1}{P_{\mathbf{Z}}(\hat{\sigma}_r^{\mathbf{Z}})^2 \langle\chi_1 \mathbf{u}_r^{\mathbf{Z}}\rangle ^2\epsilon^2}\right)$

### A. Required number of repetitions of each elemental estimation process

Table I summarizes the elemental estimation process and their required numbers of repetitions.

The factor  $\|\mathbf{X}'\|_{\mathbb{F}}/\|\mathbf{X}\|_{\mathbb{F}}$  is estimated through the measurement of the fourth register of  $|[\mathbf{X} \ \mathbf{X}']\rangle_{1:4}$ . Here, we denote a ket vector of the  $k$ -th to  $k'$ -th registers like  $|\rangle_{k:k'}$ . This estimation relies on the estimation of the measurement probabilities  $\Pr(q_4 = 0)$  and  $\Pr(q_4 = 1)$ . The error of the probability estimation decrease as the number of samples increases obeying the central limit theorem. Therefore,  $O(1/\epsilon^2)$  repetitions of the estimation process is needed to estimate the factor with precision  $\epsilon$ .

Each normalized singular value  $\hat{\sigma}$  of matrix  $\mathbf{Z}$  is encoded in the fifth register of  $|\text{SVD}(\mathbf{Z})\rangle_{1:5}$ . Measuring the fifth register, one can obtain the bit string of a singular value. Consequently, the required number of the measurement for estimating each singular value is one. Note that it is probabilistic which singular value is measured; this probabilistic nature will be considered in the next subsection.

For each left singular vector  $\mathbf{u}$ , the inner product  $\langle\chi_1|\mathbf{u}\rangle$  is estimated by the two-state SWAP test. The two-state SWAP test estimates the inner product through a measurement probability estimation. Thus  $O(1/\epsilon^2)$  repetitions of the two-state SWAP test is necessary for estimating  $\langle\chi_1|\mathbf{u}\rangle$  with precision  $\epsilon$ .

For each pair of left singular vectors  $\mathbf{u}$  and  $\mathbf{u}'$ , the inner product  $\langle\mathbf{u}|\mathbf{u}'\rangle$  is estimated by the three-state SWAP test. The three-state SWAP test estimates  $\langle\chi_1|\mathbf{u}\rangle\langle\mathbf{u}|\mathbf{u}'\rangle\langle\mathbf{u}'|\chi_1\rangle$ . Therefore, the required precision of the three-state SWAP test is  $|\langle\chi_1|\mathbf{u}\rangle||\langle\chi_1|\mathbf{u}'\rangle|\epsilon$  for estimating  $\langle\mathbf{u}|\mathbf{u}'\rangle$  with precision  $\epsilon$ . Given that the estimation error obeys the central limit theorem, the required number of the three-state SWAP test for estimating  $\langle\mathbf{u}|\mathbf{u}'\rangle$  is  $O(1/|\langle\chi_1|\mathbf{u}\rangle|^2|\langle\chi_1|\mathbf{u}'\rangle|^2\epsilon^2)$ . Likewise, for each pair of right singular vectors  $\mathbf{v}$  and  $\mathbf{v}'$ , the estimation of  $\langle\mathbf{v}|\mathbf{v}'\rangle$  requires  $O(1/|\langle\chi_2|\mathbf{v}^*\rangle|^2|\langle\chi_2|\mathbf{v}'^*\rangle|^2\epsilon^2)$  repetitions of the three-state SWAP test.

For each right singular vector  $\mathbf{v}_r^{\mathbf{Z}}$  ( $\mathbf{Z} = \mathbf{X}, \mathbf{X}'$ ,  $r = 1, \dots, R$ ), the inner product  $\langle\chi_2|\mathbf{v}_r^{\mathbf{Z}*}\rangle$  is estimated by the quantum circuit depicted in Figs. 3 and 4 of the main text. This circuit estimate  $\sqrt{P_{\mathbf{Z}}}\hat{\sigma}_r^{\mathbf{Z}}\langle\chi_1|\mathbf{u}_r^{\mathbf{Z}}\rangle\langle\chi_2|\mathbf{v}_r^{\mathbf{Z}*}\rangle$  through a probability estimation. Here,  $P_{\mathbf{Z}}$  denotes the probability of obtaining  $|\mathbf{Z}\rangle$  by measuring the fourth register of  $|[\mathbf{X} \ \mathbf{X}']\rangle$ , that is,

$$P_{\mathbf{Z}} := \frac{\|\mathbf{Z}\|_{\mathbb{F}}^2}{\|[\mathbf{X} \ \mathbf{X}']\|_{\mathbb{F}}^2}. \quad (\text{S.1})$$

Consequently, the required number of repetitions of running the circuit is  $O(1/P_{\mathbf{Z}}(\hat{\sigma}_r^{\mathbf{Z}})^2|\langle\chi_1|\mathbf{u}_r^{\mathbf{Z}}\rangle|^2\epsilon^2)$ .

### B. Required number of quantum SVDs for singular value and vector collection

The singular value estimation and the two-state and three-state SWAP tests require quantum states encoding a singular value or a singular vector. A single quantum SVD process provides a triple of a singular value and its associated left and right singular vector states at random. Furthermore, it is necessary to repeat the SWAP test for each element a certain number of times, as discussed in the previous subsection. Thus let us consider the number of quantum SVDs necessary for collecting  $m$  each of all dominant singular value and singular vector states.

Brayton [1] investigated the asymptotic behavior of the number of trials necessary to collect  $m$  copies of a set of  $n$  objects by random selection, denoted by  $E_m(n)$ . The probability of selecting the  $i$ -th object is assumed to be given by

$$p_i = \int_{(i-1)/n}^{i/n} f(s)ds, \quad (\text{S.2})$$



where the function  $f$  satisfies the following conditions:

1.  $\int_0^1 f(s)ds = 1$ .
2.  $\min f(s) = \delta > 0$ ;  $\max f(s) < \infty$ .
3.  $f(s)$  is a function of bounded variation on  $[0, 1]$ .

Brayton proved that if  $f(s) = \delta$  on a set of intervals of length  $l > 0$ , the asymptotic behavior of  $E_m(n)$  as  $n \rightarrow \infty$  is given by

$$E_m(n) = \frac{n}{\delta} \left[ \log \Gamma n + (m-1) \log \log \Gamma n + \gamma + (m-1) \log \frac{1}{\delta} + o(1) \right], \quad (\text{S.3})$$

where  $\gamma$  is the Euler–Mascheroni constant and

$$\Gamma = l \frac{\delta^{m-1}}{(m-1)!}. \quad (\text{S.4})$$

Let us define  $f$  by a piecewise constant function such that  $f(s) = np_i$  for  $(i-1)/n \leq s < i/n$ . Additionally, we denote the minimum probability of random selection by  $p_{\min}$ . In that case,  $\delta = np_{\min} \leq 1$  and  $\Gamma \leq l \leq 1$ . Therefore, the expected number of necessary trials roughly scales as

$$E_m(n) = O \left( \frac{1}{p_{\min}} \left[ \log n + (m-1) \log \frac{\log n}{np_{\min}} \right] \right). \quad (\text{S.5})$$

We can further rewrite this asymptotic equation using the maximum probability of random selection,  $p_{\max}$ , as

$$E_m(n) = O \left( \frac{p_{\max}}{p_{\min}} \left[ n \log n + n(m-1) \log \left( \frac{p_{\max}}{p_{\min}} \log n \right) \right] \right), \quad (\text{S.6})$$

because  $1 \leq np_{\max}$  holds.

In the case of the singular value and singular vector collection for matrix  $\mathbf{Z}$ , the number of objects  $n$  equals  $R$ , and the ratio of the maximum and minimum probabilities is given by

$$\frac{p_{\max}}{p_{\min}} = \frac{\max_r (\hat{\sigma}_r^{\mathbf{Z}})^2}{\min_r (\hat{\sigma}_r^{\mathbf{Z}})^2} = \left( \frac{\max_r \hat{\sigma}_r^{\mathbf{Z}}}{\min_r \hat{\sigma}_r^{\mathbf{Z}}} \right)^2. \quad (\text{S.7})$$

Let us define a parameter  $\kappa_{\mathbf{Z}}$  as

$$\kappa_{\mathbf{Z}} := \frac{\max_r \sigma_r^{\mathbf{Z}}}{\min_r \sigma_r^{\mathbf{Z}}} = \frac{\max_r \hat{\sigma}_r^{\mathbf{Z}}}{\min_r \hat{\sigma}_r^{\mathbf{Z}}}. \quad (\text{S.8})$$

The parameter  $\kappa_{\mathbf{Z}}$  is also known as the condition number of  $\mathbf{Z}$  (with rank- $R$  truncation). Using this parameter, we can write the required number of quantum SVDs for collecting  $m$  each of all dominant singular value and singular vector states of  $\mathbf{Z}$  as

$$E_m(R) = O \left( \kappa_{\mathbf{Z}}^2 [R \log R + (m-1)R \log (\kappa_{\mathbf{Z}} \log R)] \right). \quad (\text{S.9})$$

Note that since the qDMD algorithm relies on the rank- $R$  approximation of  $\hat{\mathbf{Z}}$ , the probability of selecting a singular value other than the  $R$  dominant singular values may be non-zero. However, as we determine  $R$  such that the error of the rank- $R$  approximation is less than a specified tolerance in terms of the Frobenius norm, the probability of selecting one of  $R$  dominant singular values, given by  $\sum_{r=1}^R (\hat{\sigma}_r^{\mathbf{Z}})^2$ , is  $O(1)$ . Thus we can neglect the probability of selecting other minor singular values.

### C. Required number of quantum SVDs for estimating $\tilde{\mathbf{K}}'$

Now, we evaluate the total number of quantum SVDs necessary for estimating the whole matrix  $\tilde{\mathbf{K}}'$ . We first note that the factor  $\|\mathbf{X}'\|_{\text{F}}/\|\mathbf{X}\|_{\text{F}}$  and the normalized singular value matrices  $\tilde{\Sigma}$  and  $\tilde{\Sigma}'$  can be estimated in the course of preparing singular vector states for the SWAP tests. In other words, we can include the costs of these estimations into those of preparing singular vector states. Therefore, we only consider the computational costs for the inner product estimation.

According to Table I, the required number of repetitions of the three-state SWAP test depends on an inner product between a singular vector state and a reference state. For the simplicity of the notation, let us introduce a parameter  $\zeta$  defined as

$$\zeta := \min\{\zeta_1, \zeta_2\}, \quad (\text{S.10})$$

$$\zeta_1 := \min \{ |\langle \chi_1 | \mathbf{u}_r^{\mathbf{Z}} \rangle|^2 \mid \mathbf{Z} \in \{\mathbf{X}, \mathbf{X}', [\mathbf{X} \ \mathbf{X}']\}, r \in \{1, \dots, R\} \}, \quad (\text{S.11})$$

$$\zeta_2 := \min \{ |\langle \chi_2 | \mathbf{v}_r^{\mathbf{Z}^*} \rangle|^2 \mid \mathbf{Z} \in \{\mathbf{X}, \mathbf{X}'\}, r \in \{1, \dots, R\} \}. \quad (\text{S.12})$$

Then, the required number of repetitions of the three-state SWAP test scales as  $O(1/(\zeta\epsilon)^2)$ . In addition, each singular vector is involved in  $O(R)$  different inner products to be estimated by the three-state SWAP test. Consequently, the three-state SWAP test requires  $O(R/(\zeta\epsilon)^2)$  copies of each singular vector state in total. Furthermore, the two-state SWAP test requires  $O(1/\epsilon^2)$  copies of each right singular vector state. Because  $R/\zeta^2 \geq 1$ , the total copy number of each singular vector state necessary for the two-state and three-state SWAP tests is roughly estimated as  $O(R/(\zeta\epsilon)^2)$ . Due to Eq. (S.9), we get the order estimate of the total number of quantum SVDs necessary for the SWAP tests in the qDMD algorithm:

$$O\left(\left(\frac{\kappa R}{\zeta\epsilon}\right)^2 \log(\kappa^2 \log R)\right), \quad (\text{S.13})$$

where we define  $\kappa$  by  $\max_{\mathbf{Z}} \kappa_{\mathbf{Z}}$  for brevity.

According to Table I, the total number of repetitions of the quantum circuit shown in Figs. 3 and 4 for estimating  $2R$  inner products  $\{\langle \chi_2 | \mathbf{v}_r^{\mathbf{Z}^*} \rangle\}$  is

$$O\left(\frac{\eta}{\zeta_1} \left(\frac{\kappa R}{\epsilon}\right)^2\right), \quad (\text{S.14})$$

where we define parameter  $\eta$  as

$$\eta := \frac{1}{\min\{P_{\mathbf{X}}, P_{\mathbf{X}'}\}}, \quad (\text{S.15})$$

and we use the equation

$$\frac{1}{\min_r (\hat{\sigma}_r^{\mathbf{Z}})^2} = O(R\kappa_{\mathbf{Z}}^2). \quad (\text{S.16})$$

Eq. (S.16) is equivalent to the equation  $1/p_{\min} \leq R(p_{\max}/p_{\min})$ , which is used to derive Eq. (S.9) in the previous subsection. Since the circuit contains one quantum SVD process, this total number of repetitions given by Eq. (S.14) equals the total number of quantum SVDs for estimating  $\{\langle \chi_2 | \mathbf{v}_r^{\mathbf{Z}^*} \rangle\}$ . Additionally, we note that  $\eta$  is  $O(1)$  due to the following reason: Because  $\mathbf{X}' \approx (\mathbf{1} + \Delta t \mathbf{A})\mathbf{X}$ ,  $\|\mathbf{X}'\|_{\text{F}}/\|\mathbf{X}\|_{\text{F}} = 1 + O(\Delta t)$ ; consequently, it is expected that  $P_{\mathbf{X}'} = P_{\mathbf{X}} + O(\Delta t)$ , which leads to  $\eta = O(1)$ . Due to the facts that  $\eta = O(1)$  and that  $\zeta \leq \zeta_1 < 1$ , the cost estimate in Eq. (S.14) is less than that in Eq. (S.13).

In summary, the number of quantum SVDs necessary for estimating  $\tilde{\mathbf{K}}'$  with precision  $\epsilon$  is

$$O\left(\left(\frac{\kappa R}{\zeta\epsilon}\right)^2 \log(\kappa^2 \log R)\right). \quad (\text{S.17})$$

Because one quantum SVD process requires  $O(1/\epsilon^2)$  copies of a data matrix [2], the required number of differential equation solutions is

$$O\left(\frac{1}{\epsilon^4} \left(\frac{\kappa R}{\zeta}\right)^2 \log(\kappa^2 \log R)\right). \quad (\text{S.18})$$

The gate complexity is larger than the required number of differential equation solutions by a factor of  $T$  poly  $\log(NM/\epsilon)$ .

## II. REFERENCE STATE PREPARATION FOR THE INNER PRODUCT ESTIMATION

One may use any reference states  $|\chi_1\rangle$  and  $|\chi_2\rangle$  provided that  $\langle\chi_1|\mathbf{u}\rangle \neq 0$  and  $\langle\chi_2|\mathbf{v}^*\rangle \neq 0$  for all relevant left and right singular vectors  $\mathbf{u}$  and  $\mathbf{v}$ . This condition is the necessary and sufficient condition so that the inner product estimation through the three-state SWAP test is possible. Regardless of the choice of  $|\chi_1\rangle$  and  $|\chi_2\rangle$ , estimates of  $\tilde{\mathbf{K}}'$  are identical within a tolerant error. However, the choice of  $|\chi_1\rangle$  and  $|\chi_2\rangle$  affects the algorithm's efficiency: the computational complexity of estimating  $\tilde{\mathbf{K}}'$  is influenced by the choice of  $|\chi_1\rangle$  and  $|\chi_2\rangle$  through the parameter  $\zeta$ , as discussed in the previous section; the larger  $\zeta$  is, the smaller the required number of quantum SVDs is. Moreover, if the reference state preparation has a runtime greater than  $O(\text{poly log } N)$ , the qDMD algorithm cannot achieve an exponential speedup with respect to  $N$  in total.

In this section, we present an example of quantum procedures preparing  $|\chi_1\rangle$  and  $|\chi_2\rangle$ . The quantum circuits of these procedures can be constructed and executed in  $O(\text{poly log } N)$  time, ensuring that  $1/\zeta = O(\text{poly } R)$ . Therefore, this example theoretically guarantees that the qDMD algorithm achieves an exponential speedup with respect to  $N$  in estimating  $\tilde{\mathbf{K}}'$ . Additionally, we remark on other possible methods of the reference state preparation at the end of this section.

### A. Choice of $|\chi_1\rangle$ and $|\chi_2\rangle$

We define  $|\chi_1\rangle$  such that  $1/\zeta_1 = O(\text{poly } R)$ . Specifically, it is designed here to satisfy the following conditions:

$$|\langle\chi_1|\mathbf{u}_r^{[\mathbf{X} \ \mathbf{X}']}\rangle|^2 = \Omega\left(\frac{1}{R}\right), \quad (\text{S.19})$$

$$|\langle\chi_1|\mathbf{u}_r^{\mathbf{X}}\rangle|^2 = \Omega\left(\frac{1}{R^2}\right), \quad (\text{S.20})$$

$$|\langle\chi_1|\mathbf{u}_r^{\mathbf{X}'}\rangle|^2 = \Omega\left(\frac{1}{R^3}\right), \quad (\text{S.21})$$

for any  $r \in \{1, 2, \dots, R\}$ . Here, the  $\Omega$ -symbol signifies an asymptotic lower bound.

Initially, we construct a quantum state  $|\chi_1^{(0)}\rangle$  such that  $|\langle\chi_1^{(0)}|\mathbf{u}_r^{[\mathbf{X} \ \mathbf{X}']}\rangle|^2 = \Omega(1/R)$  for any  $r \in \{1, 2, \dots, R\}$ . The superposition of all left singular vector states of  $[\mathbf{X} \ \mathbf{X}']$  with equal weights satisfies this condition. Thus we define  $|\chi_1^{(0)}\rangle$  as

$$|\chi_1^{(0)}\rangle := \frac{1}{\sqrt{R}} \sum_{r=1}^R |\mathbf{u}_r^{[\mathbf{X} \ \mathbf{X}']}\rangle. \quad (\text{S.22})$$

Next, we modify  $|\chi_1^{(0)}\rangle$  to a quantum state  $|\chi_1^{(1)}\rangle$  that satisfies  $|\langle\chi_1^{(1)}|\mathbf{u}_r^{\mathbf{X}}\rangle|^2 = \Omega(1/R^2)$  as well as  $|\langle\chi_1^{(1)}|\mathbf{u}_r^{[\mathbf{X} \ \mathbf{X}']}\rangle|^2 = \Omega(1/R)$  for any  $r \in \{1, 2, \dots, R\}$ . Let  $S_1^{(1)}$  be a set of left singular vector states of  $\mathbf{X}$  defined by

$$S_1^{(1)} := \left\{ |\mathbf{u}_r^{\mathbf{X}}\rangle \mid r \in \{1, 2, \dots, R\}, |\langle\chi_1^{(0)}|\mathbf{u}_r^{\mathbf{X}}\rangle| \leq \frac{1}{4R} \right\}. \quad (\text{S.23})$$

This set is a collection of  $|\mathbf{u}_r^{\mathbf{X}}\rangle$  whose overlap with the temporary reference state  $|\chi_1^{(0)}\rangle$ , i.e.,  $|\langle\chi_1^{(0)}|\mathbf{u}_r^{\mathbf{X}}\rangle|^2$ , is small compared with  $1/R^2$ . To ensure that  $|\mathbf{u}_r^{\mathbf{X}}\rangle \in S_1^{(1)}$  has  $\Omega(1/R^2)$  overlap with the reference state, we add a correction term  $|\phi_1^{(1)}\rangle$  to the temporary reference state  $|\chi_1^{(0)}\rangle$ :

$$|\phi_1^{(1)}\rangle := \frac{1}{\sqrt{|S_1^{(1)}|}} \sum_{|\mathbf{u}_r^{\mathbf{X}}\rangle \in S_1^{(1)}} |\mathbf{u}_r^{\mathbf{X}}\rangle, \quad (\text{S.24})$$

and

$$|\chi_1^{(1)}\rangle := \mathcal{C}_1^{(1)} \left[ |\chi_1^{(0)}\rangle + \frac{1}{2\sqrt{R}} |\phi_1^{(1)}\rangle \right]. \quad (\text{S.25})$$

Here,  $\mathcal{C}_1^{(1)}$  is the normalizing constant. The coefficient  $1/2\sqrt{R}$  of  $|\phi_1^{(1)}\rangle$  is introduced to ensure that this correction is small enough not to violate the condition  $|\langle\chi_1^{(1)}|\mathbf{u}_r^{[\mathbf{X} \ \mathbf{X}']}\rangle|^2 = \Omega(1/R)$ . We can confirm that  $|\chi_1^{(1)}\rangle$  satisfies the

mentioned conditions on inner products as follows: The normalizing constant  $\mathcal{C}_1^{(1)}$  is  $\Omega(1)$  because

$$\begin{aligned} \mathcal{C}_1^{(1)} &= \frac{1}{\| |\chi_1^{(0)}\rangle + \frac{1}{2\sqrt{R}} |\phi_1^{(1)}\rangle \|} \\ &\geq \frac{1}{\| |\chi_1^{(0)}\rangle \| + \frac{1}{2\sqrt{R}} \| |\phi_1^{(1)}\rangle \|} \\ &= \frac{1}{1 + \frac{1}{2\sqrt{R}}} \\ &\geq \frac{2}{3}. \end{aligned} \tag{S.26}$$

For any  $|\mathbf{u}_r^{[\mathbf{X} \ \mathbf{X}']}\rangle$ ,

$$\begin{aligned} |\langle \chi_1^{(1)} | \mathbf{u}_r^{[\mathbf{X} \ \mathbf{X}']}\rangle| &\geq \mathcal{C}_1^{(1)} \left[ |\langle \chi_1^{(0)} | \mathbf{u}_r^{[\mathbf{X} \ \mathbf{X}']}\rangle| - \frac{1}{2\sqrt{R}} |\langle \phi_1^{(1)} | \mathbf{u}_r^{[\mathbf{X} \ \mathbf{X}']}\rangle| \right] \\ &\geq \frac{2}{3} \left[ \frac{1}{\sqrt{R}} - \frac{1}{2\sqrt{R}} \right] \\ &= \frac{1}{3\sqrt{R}}. \end{aligned} \tag{S.27}$$

The first inequality follows from the triangle inequality. Likewise, for any  $|\mathbf{u}_r^{\mathbf{X}}\rangle \in S_1^{(1)}$ ,

$$\begin{aligned} |\langle \chi_1^{(1)} | \mathbf{u}_r^{\mathbf{X}}\rangle| &\geq \mathcal{C}_1^{(1)} \left[ \frac{1}{2\sqrt{R}} |\langle \phi_1^{(1)} | \mathbf{u}_r^{\mathbf{X}}\rangle| - |\langle \chi_1^{(0)} | \mathbf{u}_r^{\mathbf{X}}\rangle| \right] \\ &\geq \frac{2}{3} \left[ \frac{1}{2\sqrt{R}} \frac{1}{\sqrt{|S_1^{(1)}|}} - \frac{1}{4R} \right] \\ &\geq \frac{2}{3} \left[ \frac{1}{2\sqrt{R}} \frac{1}{\sqrt{R}} - \frac{1}{4R} \right] \\ &= \frac{1}{6R}. \end{aligned} \tag{S.28}$$

Any  $|\mathbf{u}_r^{\mathbf{X}}\rangle \notin S_1^{(1)}$  is orthogonal to  $|\phi_1^{(1)}\rangle \in \text{span } S_1^{(1)}$ . Consequently, for any  $|\mathbf{u}_r^{\mathbf{X}}\rangle \notin S_1^{(1)}$ ,

$$|\langle \chi_1^{(1)} | \mathbf{u}_r^{\mathbf{X}}\rangle| = \mathcal{C}_1^{(1)} |\langle \chi_1^{(0)} | \mathbf{u}_r^{\mathbf{X}}\rangle| \geq \frac{2}{3} \frac{1}{4R} = \frac{1}{6R}. \tag{S.29}$$

Therefore,  $|\chi_1^{(1)}\rangle$  satisfies  $|\langle \chi_1^{(1)} | \mathbf{u}_r^{[\mathbf{X} \ \mathbf{X}']}\rangle|^2 = \Omega(1/R)$  and  $|\langle \chi_1^{(1)} | \mathbf{u}_r^{\mathbf{X}}\rangle|^2 = \Omega(1/R^2)$  for any  $r \in \{1, 2, \dots, R\}$ .

Finally, we modify  $|\chi_1^{(1)}\rangle$  to a quantum state  $|\chi_1^{(2)}\rangle$  that also satisfies  $|\langle \chi_1^{(1)} | \mathbf{u}_r^{\mathbf{X}'}\rangle|^2 = \Omega(1/R^3)$ . Let us define  $S_1^{(2)}$  as

$$S_1^{(2)} := \left\{ |\mathbf{u}_r^{\mathbf{X}'}\rangle \mid r \in \{1, 2, \dots, R\}, |\langle \chi_1^{(1)} | \mathbf{u}_r^{\mathbf{X}'}\rangle| \leq \frac{1}{14R\sqrt{R}} \right\}. \tag{S.30}$$

Then, we define  $|\chi_1^{(2)}\rangle$  by adding a correction term  $|\phi_1^{(2)}\rangle$  to  $|\chi_1^{(1)}\rangle$ :

$$|\phi_1^{(2)}\rangle := \frac{1}{\sqrt{|S_1^{(2)}|}} \sum_{|\mathbf{u}_r^{\mathbf{X}'}\rangle \in S_1^{(2)}} |\mathbf{u}_r^{\mathbf{X}'}\rangle, \tag{S.31}$$

and

$$|\chi_1^{(2)}\rangle := \mathcal{C}_1^{(2)} \left[ |\chi_1^{(1)}\rangle + \frac{1}{7R} |\phi_1^{(2)}\rangle \right], \tag{S.32}$$

where  $\mathcal{C}_1^{(2)}$  is the normalizing constant. We can confirm that  $|\chi_1^{(2)}\rangle$  satisfies the aforementioned conditions on inner products as follows: The normalizing constant  $\mathcal{C}_1^{(2)}$  is  $\Omega(1)$  because

$$\begin{aligned}\mathcal{C}_1^{(2)} &= \frac{1}{\| |\chi_1^{(1)}\rangle + \frac{1}{7R} |\phi_1^{(2)}\rangle \|} \\ &\geq \frac{1}{\| |\chi_1^{(1)}\rangle \| + \frac{1}{7R} \| |\phi_1^{(2)}\rangle \|} \\ &\geq \frac{1}{1 + \frac{1}{7R}} \\ &\geq \frac{7}{8}.\end{aligned}\tag{S.33}$$

For any  $|\mathbf{u}_r^{[\mathbf{X}, \mathbf{X}']}\rangle$ ,

$$\begin{aligned}|\langle \chi_1^{(2)} | \mathbf{u}_r^{[\mathbf{X}, \mathbf{X}']}\rangle| &\geq \mathcal{C}_1^{(2)} \left[ |\langle \chi_1^{(1)} | \mathbf{u}_r^{[\mathbf{X}, \mathbf{X}']}\rangle| - \frac{1}{7R} |\langle \phi_1^{(2)} | \mathbf{u}_r^{[\mathbf{X}, \mathbf{X}']}\rangle| \right] \\ &\geq \frac{7}{8} \left[ \frac{1}{3\sqrt{R}} - \frac{1}{7R} \right] \\ &\geq \frac{7}{8} \left[ \frac{1}{3\sqrt{R}} - \frac{1}{7\sqrt{R}} \right] \\ &= \frac{1}{6\sqrt{R}}.\end{aligned}\tag{S.34}$$

For any  $|\mathbf{u}_r^{\mathbf{X}}\rangle$ ,

$$\begin{aligned}|\langle \chi_1^{(2)} | \mathbf{u}_r^{\mathbf{X}}\rangle| &\geq \mathcal{C}_1^{(2)} \left[ |\langle \chi_1^{(1)} | \mathbf{u}_r^{\mathbf{X}}\rangle| - \frac{1}{7R} |\langle \phi_1^{(2)} | \mathbf{u}_r^{\mathbf{X}}\rangle| \right] \\ &\geq \frac{7}{8} \left[ \frac{1}{6R} - \frac{1}{7R} \right] \\ &= \frac{1}{48R}.\end{aligned}\tag{S.35}$$

For any  $|\mathbf{u}_r^{\mathbf{X}'}\rangle \in S_1^{(2)}$ ,

$$\begin{aligned}|\langle \chi_1^{(2)} | \mathbf{u}_r^{\mathbf{X}'}\rangle| &\geq \mathcal{C}_1^{(2)} \left[ \frac{1}{7R} |\langle \phi_1^{(2)} | \mathbf{u}_r^{\mathbf{X}'}\rangle| - |\langle \chi_1^{(1)} | \mathbf{u}_r^{\mathbf{X}'}\rangle| \right] \\ &\geq \frac{7}{8} \left[ \frac{1}{7R} \frac{1}{\sqrt{|S_1^{(2)}|}} - \frac{1}{14R\sqrt{R}} \right] \\ &\geq \frac{7}{8} \left[ \frac{1}{7R} \frac{1}{\sqrt{R}} - \frac{1}{14R\sqrt{R}} \right] \\ &= \frac{1}{16R\sqrt{R}}.\end{aligned}\tag{S.36}$$

For any  $|\mathbf{u}_r^{\mathbf{X}'}\rangle \notin S_1^{(2)}$ ,

$$|\langle \chi_1^{(2)} | \mathbf{u}_r^{\mathbf{X}'}\rangle| = \mathcal{C}_1^{(2)} |\langle \chi_1^{(1)} | \mathbf{u}_r^{\mathbf{X}'}\rangle| \geq \frac{7}{8} \frac{1}{14R\sqrt{R}} = \frac{1}{16R\sqrt{R}}.\tag{S.37}$$

Therefore,  $|\chi_1^{(2)}\rangle$  defined here can be employed as  $|\chi_1\rangle$  that satisfies  $1/\zeta_1 = O(\text{poly } R)$ .

Likewise, a reference state  $|\chi_2\rangle$  that satisfies  $1/\zeta_2 = O(\text{poly } R)$  can be defined as

$$|\chi_2\rangle := \mathcal{C}_2^{(1)} \left[ |\chi_2^{(0)}\rangle + \frac{1}{2\sqrt{R}} |\phi_2^{(1)}\rangle \right],\tag{S.38}$$

where  $\mathcal{C}_2^{(1)}$  is the normalizing constant,

$$|\chi_2^{(0)}\rangle := \frac{1}{\sqrt{R}} \sum_{r=1}^R |\mathbf{v}_r^{\mathbf{X}^*}\rangle, \quad (\text{S.39})$$

$$|\phi_2^{(1)}\rangle := \frac{1}{\sqrt{|S_2^{(1)}|}} \sum_{|\mathbf{v}_r^{\mathbf{X}'^*}\rangle \in S_2^{(1)}} |\mathbf{v}_r^{\mathbf{X}'^*}\rangle, \quad (\text{S.40})$$

and

$$S_2^{(1)} := \left\{ |\mathbf{v}_r^{\mathbf{X}'^*}\rangle \mid r \in \{1, 2, \dots, R\}, |\langle \chi_2^{(0)} | \mathbf{v}_r^{\mathbf{X}'^*} \rangle| \leq \frac{1}{4R} \right\}. \quad (\text{S.41})$$

Note that the qDMD algorithm does not need to estimate  $\langle \chi_2 | \mathbf{v}_r^{\mathbf{X}^{\mathbf{X}'^*}} \rangle$ . Consequently, the above definition of  $|\chi_2\rangle$  does not contain  $|\mathbf{v}_r^{\mathbf{X}^{\mathbf{X}'^*}}\rangle$ .

## B. Computation of $|\chi_1\rangle$ and $|\chi_2\rangle$

We present quantum circuits that generate  $|\chi_1\rangle$  and  $|\chi_2\rangle$  defined in the previous subsection.

Initially, we perform pure-state tomography [3] to estimate all right singular vector states of  $\mathbf{X}$ ,  $\mathbf{X}'$ , and  $[\mathbf{X} \ \mathbf{X}']$ . The pure-state tomography requires an  $O(M)$  runtime for each right singular vector state of  $M$  dimensions. Subsequently, for each right singular vector state  $|\mathbf{v}^*\rangle$ , we construct a quantum circuit  $U_{\mathbf{v}^*}$  such that  $U_{\mathbf{v}^*} |0\rangle = |\mathbf{v}^*\rangle$ <sup>1</sup>. When the classical data of the amplitudes of  $|\mathbf{v}^*\rangle$  is given, such a quantum circuit can be implemented with a gate complexity of  $O(\text{poly log } M)$  [4, 5].

Next, we compute  $|\chi_1^{(0)}\rangle$  with the following steps: (1) Prepare  $|\text{SVD}([\mathbf{X} \ \hat{\mathbf{X}}']]\rangle$ . (2) Uncompute the second to fourth registers of  $|\text{SVD}([\mathbf{X} \ \hat{\mathbf{X}}']]\rangle$  by controlled- $U_{\mathbf{v}_r^{\mathbf{X} \ \mathbf{X}'^*}}^\dagger$  operations:

$$\begin{aligned} |\text{SVD}([\mathbf{X} \ \hat{\mathbf{X}}']]\rangle &= \sum_{r=1}^R \hat{\sigma}_r^{[\mathbf{X} \ \mathbf{X}']} |\mathbf{u}_r^{[\mathbf{X} \ \mathbf{X}']}\rangle_1 |\mathbf{v}_r^{[\mathbf{X} \ \mathbf{X}'^*]}\rangle_{234} |(\hat{\sigma}_r^{[\mathbf{X} \ \mathbf{X}']})^2\rangle_5 \\ &\mapsto \sum_{r=1}^R \hat{\sigma}_r^{[\mathbf{X} \ \mathbf{X}']} |\mathbf{u}_r^{[\mathbf{X} \ \mathbf{X}']}\rangle_1 U_{\mathbf{v}_r^{\mathbf{X} \ \mathbf{X}'^*}}^\dagger |\mathbf{v}_r^{[\mathbf{X} \ \mathbf{X}'^*]}\rangle_{234} |(\hat{\sigma}_r^{[\mathbf{X} \ \mathbf{X}']})^2\rangle_5 \\ &= \sum_{r=1}^R \hat{\sigma}_r^{[\mathbf{X} \ \mathbf{X}']} |\mathbf{u}_r^{[\mathbf{X} \ \mathbf{X}']}\rangle_1 |0\rangle_{234} |(\hat{\sigma}_r^{[\mathbf{X} \ \mathbf{X}']})^2\rangle_5. \end{aligned} \quad (\text{S.42})$$

Here, each  $U_{\mathbf{v}_r^{\mathbf{X} \ \mathbf{X}'^*}}^\dagger$  is applied to the second to fourth registers of  $|\text{SVD}([\mathbf{X} \ \hat{\mathbf{X}}']]\rangle$  conditionally on the fifth register. (3) Add an ancilla qubit (the sixth register). (4) Compute the following state by controlled rotations of the ancilla qubit conditionally on the fifth register:

$$\sum_{r=1}^R \hat{\sigma}_r^{[\mathbf{X} \ \mathbf{X}']} |\mathbf{u}_r^{[\mathbf{X} \ \mathbf{X}']}\rangle_1 |0\rangle_{234} |(\hat{\sigma}_r^{[\mathbf{X} \ \mathbf{X}']})^2\rangle_5 \left[ \frac{a_0}{\hat{\sigma}_r^{[\mathbf{X} \ \mathbf{X}']}\sqrt{R}} |0\rangle_6 + \sqrt{1 - \left| \frac{a_0}{\hat{\sigma}_r^{[\mathbf{X} \ \mathbf{X}']}\sqrt{R}} \right|^2} |1\rangle_6 \right], \quad (\text{S.43})$$

where  $a_0$  is a constant such that

$$\frac{a_0}{\hat{\sigma}_r^{[\mathbf{X} \ \mathbf{X}']}\sqrt{R}} \leq 1, \quad \forall r \in \{1, 2, \dots, R\}. \quad (\text{S.44})$$

This condition is the necessary and sufficient condition for the controlled rotations to be possible and is equivalent to

$$a_0 \leq \sqrt{R} \min_r \hat{\sigma}_r^{[\mathbf{X} \ \mathbf{X}']}. \quad (\text{S.45})$$

<sup>1</sup> Because the pure-state tomography can not determine the global phase of a right singular vector state, the unitary gate  $U_{\mathbf{v}^*}$  may act as  $U_{\mathbf{v}^*} |0\rangle = \exp(-i\varphi) |\mathbf{v}^*\rangle$  where  $\varphi$  signifies the unknown global phase. This unknown phase factor will change the relative phase of the associated left and right singular vector states in the computed reference states. However, such phase factor does not violate the condition  $1/\zeta = O(\text{poly } R)$  proven in the previous subsection. Thus, we omit the phase factor for simplicity in this section.

(5) Uncompute the fifth register by the inverse unitary transform of the quantum SVD process. Specifically, the inverse process consists of the inverse quantum Fourier transform of the fifth register and the density matrix exponentiation multiplying  $\exp(-i \text{tr}_{234}(|[\mathbf{X} \hat{\mathbf{X}}']\rangle\langle[\mathbf{X} \hat{\mathbf{X}}']|)t)$  to the first register conditioned on the fifth register. Here,  $\text{tr}_{234}$  denotes the partial trace with respect to the second to fourth registers. See [6] for the details of the quantum SVD process. (6) Measure the second to sixth registers. If all measured values are zero, we obtain  $|\chi_1^{(0)}\rangle_1|0\rangle_{2:6}$ . The success probability is  $a_0^2$ . When  $\sqrt{R} \min_r \hat{\sigma}_r^{[\mathbf{X} \mathbf{X}']}$  is employed as  $a_0$ , an asymptotic lower bound of the success probability can be evaluated as

$$a_0^2 = R(\min_r \hat{\sigma}_r^{[\mathbf{X} \mathbf{X}']})^2 = \Omega\left(R \frac{1}{R\kappa_{[\mathbf{X} \mathbf{X}']}}\right) = \Omega\left(\frac{1}{\kappa^2}\right). \quad (\text{S.46})$$

Here,  $\kappa_{\mathbf{Z}}$  denotes the condition number of  $\mathbf{Z}$  ( $\mathbf{Z} = \mathbf{X}, \mathbf{X}', [\mathbf{X} \mathbf{X}']$ ) defined in Eq. (S.8),  $\kappa := \max_{\mathbf{Z}} \kappa_{\mathbf{Z}}$ , and we use Eq. (S.16) to derive the lower bound. In summary, we can compute  $|\chi_1^{(0)}\rangle$  by  $O(\kappa^2 R)$  controlled- $U_{\mathbf{v}^*}^\dagger$  operations and  $O(\kappa^2)$  inverse quantum SVD operations.

Having established the computation for  $|\chi_1^{(0)}\rangle$ , we next address the computation for  $|\chi_1^{(1)}\rangle$ : (1) Determine whether each  $|\mathbf{u}_r^{\mathbf{X}}\rangle$  belongs to  $S_1^{(1)}$  using the two-state SWAP test between  $|\chi_1^{(0)}\rangle$  and  $|\mathbf{u}_r^{\mathbf{X}}\rangle$ . If  $|S_1^{(1)}| = 0$ , then  $|\chi_1^{(1)}\rangle = |\chi_1^{(0)}\rangle$ . Thus we consider the case that  $|S_1^{(1)}| \geq 1$  below. (2) Prepare the following state:

$$|[\mathbf{X} \hat{\mathbf{X}}']\rangle_{1:4} |0\rangle_5 |0\rangle_6 \left[ \frac{1}{\sqrt{2}} (|0\rangle_7 + |1\rangle_7) \right], \quad (\text{S.47})$$

where the fifth register is an ancilla register for indicating singular values, and the sixth and seventh registers are one-qubit ancilla registers. Note that  $|[\mathbf{X} \hat{\mathbf{X}}']\rangle_{1:4}$  can be written as

$$|[\mathbf{X} \hat{\mathbf{X}}']\rangle_{1:4} = \sqrt{P_{\mathbf{X}}} |\hat{\mathbf{X}}\rangle_{123} |0\rangle_4 + \sqrt{P_{\mathbf{X}'}} |\hat{\mathbf{X}}'\rangle_{123} |1\rangle_4, \quad (\text{S.48})$$

with

$$P_{\mathbf{Z}} = \frac{\|\mathbf{Z}\|_{\mathbb{F}}^2}{\|[\mathbf{X} \mathbf{X}']\|_{\mathbb{F}}^2}, \quad \mathbf{Z} \in \{\mathbf{X}, \mathbf{X}'\}. \quad (\text{S.49})$$

Thus the prepared state is

$$\frac{1}{\sqrt{2}} |[\mathbf{X} \hat{\mathbf{X}}']\rangle_{1:4} |0\rangle_5 |0\rangle_6 |0\rangle_7 + \frac{1}{\sqrt{2}} \left[ \sqrt{P_{\mathbf{X}}} |\hat{\mathbf{X}}\rangle_{123} |0\rangle_4 |0\rangle_5 |0\rangle_6 |1\rangle_7 + \sqrt{P_{\mathbf{X}'}} |\hat{\mathbf{X}}'\rangle_{123} |1\rangle_4 |0\rangle_5 |0\rangle_6 |1\rangle_7 \right]. \quad (\text{S.50})$$

(3) Perform the steps 2–5 of computing  $|\chi_1^{(0)}\rangle$  described above conditionally on the seventh register to get

$$\frac{1}{\sqrt{2}} a_0 |\chi_1^{(0)}\rangle_1 |0\rangle_{2:6} |0\rangle_7 + \frac{1}{\sqrt{2}} \sqrt{P_{\mathbf{X}}} |\hat{\mathbf{X}}\rangle_{123} |0\rangle_4 |0\rangle_5 |0\rangle_6 |1\rangle_7 + \dots \quad (\text{S.51})$$

In the computation for  $|\chi_1^{(1)}\rangle$ , the constant  $a_0$  is specified as

$$a_0 = \min \left\{ \sqrt{R} \min_r \hat{\sigma}_r^{[\mathbf{X} \mathbf{X}']}, 2\sqrt{P_{\mathbf{X}} R |S_1^{(1)}|} \min_{r \in \text{ind } S_1^{(1)}} \hat{\sigma}_r^{\mathbf{X}} \right\}, \quad (\text{S.52})$$

where

$$\text{ind } S_1^{(1)} := \left\{ r \in \{1, 2, \dots, R\} \mid |\mathbf{u}_r^{\mathbf{X}}\rangle \in S_1^{(1)} \right\}. \quad (\text{S.53})$$

The reason of this specific choice is clarified in the next step. (4) In a similar way to computing  $|\chi_1^{(0)}\rangle$ , compute  $|\phi_1^{(1)}\rangle$  conditionally on the fourth and seventh register:

$$\frac{1}{\sqrt{2}} a_0 |\chi_1^{(0)}\rangle_1 |0\rangle_{2:6} |0\rangle_7 + \frac{1}{\sqrt{2}} \sqrt{P_{\mathbf{X}}} a_1 |\phi_1^{(1)}\rangle_1 |0\rangle_{2:6} |1\rangle_7 + \dots \quad (\text{S.54})$$

Here,  $a_1$  is a constant related to controlled-rotations and needs to satisfy

$$a_1 \leq \sqrt{|S_1^{(1)}|} \min_{r \in \text{ind } S_1^{(1)}} \hat{\sigma}_r^{\mathbf{X}}. \quad (\text{S.55})$$

In the present computation, we choose  $a_1$  as

$$a_1 = \frac{a_0}{2\sqrt{P_{\mathbf{X}}R}}. \quad (\text{S.56})$$

This choice is possible owing to the aforementioned choice of  $a_0$ . Consequently, we have the following state:

$$\frac{1}{\sqrt{2}}a_0 \left[ |\chi_1^{(0)}\rangle_1 |0\rangle_{2:6} |0\rangle_7 + \frac{1}{2\sqrt{R}} |\phi_1^{(1)}\rangle_1 |0\rangle_{2:6} |1\rangle_7 \right] + \dots \quad (\text{S.57})$$

(5) Apply the Hadamard gate to the seventh register to get

$$\frac{1}{2}a_0 \left[ |\chi_1^{(0)}\rangle_1 + \frac{1}{2\sqrt{R}} |\phi_1^{(1)}\rangle_1 \right] |0\rangle_{2:7} + \dots \quad (\text{S.58})$$

(6) Measure the second to seventh registers. If all measured values are zero, we obtain  $|\chi_1^{(1)}\rangle_1 |0\rangle_{2:7}$ . The success probability is  $(a_0/2\mathcal{C}_1^{(1)})^2$ . A lower bound of this probability can be evaluated as

$$\begin{aligned} \left( \frac{a_0}{2\mathcal{C}_1^{(1)}} \right)^2 &\geq \frac{P_{\mathbf{X}}R \min_{\mathbf{Z}} \min_r (\hat{\sigma}_r^{\mathbf{Z}})^2}{4} \left[ \|\chi_1^{(0)}\| - \frac{1}{2\sqrt{R}} \|\phi_1^{(1)}\| \right]^2 \\ &= \Omega \left( \frac{1}{\eta\kappa^2} \right). \end{aligned} \quad (\text{S.59})$$

Therefore, we can compute  $|\chi_1^{(1)}\rangle$  by  $O(\eta\kappa^2 R)$  controlled- $U_{v^*}^\dagger$  operations and  $O(\eta\kappa^2)$  inverse quantum SVD operations.

The reference state  $|\chi_1\rangle$  now can be computed as follows: (1) In a similar way of computing  $|\chi_1^{(1)}\rangle$ , compute

$$\begin{aligned} &\frac{1}{\sqrt{2}}a_0 |\chi_1^{(0)}\rangle_1 |0\rangle_{23} |0\rangle_4 |0\rangle_5 |0\rangle_6 |0\rangle_7 \\ &+ \frac{1}{\sqrt{2}}\sqrt{P_{\mathbf{X}}}a_1 |\phi_1^{(1)}\rangle_1 |0\rangle_{23} |0\rangle_4 |0\rangle_5 |0\rangle_6 |1\rangle_7 \\ &+ \frac{1}{\sqrt{2}}\sqrt{P_{\mathbf{X}'}}a_2 |\phi_1^{(2)}\rangle_1 |0\rangle_{23} |1\rangle_4 |0\rangle_5 |0\rangle_6 |1\rangle_7 + \dots \end{aligned} \quad (\text{S.60})$$

Here, we define the constants  $a_0$ ,  $a_1$ , and  $a_2$  as

$$a_0 = \min \left\{ \sqrt{R} \min_r \hat{\sigma}_r^{\mathbf{X}'} , \sqrt{2P_{\mathbf{X}}R} |S_1^{(1)}| \min_{r \in \text{ind } S_1^{(1)}} \hat{\sigma}_r^{\mathbf{X}} , \sqrt{\frac{(7\mathcal{C}_1^{(1)})^2 P_{\mathbf{X}'} R^2 |S_1^{(2)}|}{2}} \min_{r \in \text{ind } S_1^{(2)}} \hat{\sigma}_r^{\mathbf{X}'} \right\}, \quad (\text{S.61})$$

$$a_1 = a_0 \sqrt{\frac{1}{2P_{\mathbf{X}}R}}, \quad (\text{S.62})$$

$$a_2 = a_0 \sqrt{\frac{2}{(7\mathcal{C}_1^{(1)})^2 P_{\mathbf{X}'} R^2}}, \quad (\text{S.63})$$

where

$$\text{ind } S_1^{(2)} := \left\{ r \in \{1, 2, \dots, R\} \mid |\mathbf{u}_r^{\mathbf{X}'}\rangle \in S_1^{(2)} \right\}. \quad (\text{S.64})$$

Note that  $S_1^{(2)}$  can be determined by the two-state SWAP test between  $|\chi_1^{(1)}\rangle$  and  $|\mathbf{u}_r^{\mathbf{X}'}\rangle$  and that the value of  $\mathcal{C}_1^{(1)}$  can be estimated through the success probability of computing  $|\chi_1^{(1)}\rangle$ . Consequently, we have the following state:

$$\frac{a_0}{\sqrt{2}} |\chi_1^{(0)}\rangle_1 |0\rangle_{2:6} |0\rangle_7 + a_0 \left[ \frac{1}{2\sqrt{R}} |\phi_1^{(1)}\rangle_1 |0\rangle_{23} |0\rangle_4 |0\rangle_{56} |1\rangle_7 + \frac{1}{7\mathcal{C}_1^{(1)}R} |\phi_1^{(2)}\rangle_1 |0\rangle_{23} |1\rangle_4 |0\rangle_{56} |1\rangle_7 \right] + \dots \quad (\text{S.65})$$

(2) Apply the Hadamard gate to the fourth register conditionally on the seventh register to get

$$\frac{a_0}{\sqrt{2}} \left[ |\chi_1^{(0)}\rangle_1 |0\rangle_{2:6} |0\rangle_7 + \frac{1}{2\sqrt{R}} |\phi_1^{(1)}\rangle_1 |0\rangle_{2:6} |1\rangle_7 + \frac{1}{7\mathcal{C}_1^{(1)}R} |\phi_1^{(2)}\rangle_1 |0\rangle_{2:6} |1\rangle_7 \right] + \dots \quad (\text{S.66})$$



(3) Apply the Hadamard gate to the seventh register to get

$$\frac{a_0}{2\mathcal{C}_1^{(1)}} \left[ \mathcal{C}_1^{(1)} \left( |\chi_1^{(0)}\rangle_1 + \frac{1}{2\sqrt{R}} |\phi_1^{(1)}\rangle_1 \right) + \frac{1}{7R} |\phi_1^{(2)}\rangle_1 \right] |0\rangle_{2:7} + \dots \quad (\text{S.67})$$

(4) Measure the second to seventh registers. If all measured values are zero, we obtain  $|\chi_1\rangle_1|0\rangle_{2:7}$ . The success probability is  $(a_0/\mathcal{C}_1^{(2)}\mathcal{C}_1^{(1)})^2$ , which is  $\Omega(1/\eta\kappa^2)$ . Therefore, we can compute  $|\chi_1\rangle$  by  $O(\eta\kappa^2R)$  controlled- $U_{\mathbf{v}^*}^\dagger$  operations and  $O(\eta\kappa^2)$  inverse quantum SVD operations.

Next, let us consider how to generate  $|\chi_2^{(0)}\rangle$ : (1) Prepare the following state:

$$\frac{1}{\sqrt{R}} \sum_{r=1}^R |0\rangle_{23} |(\hat{\sigma}_r^{\mathbf{X}})^2\rangle_5. \quad (\text{S.68})$$

(2) Apply  $U_{\mathbf{v}_r^{\mathbf{X}^*}}$  conditionally on the fifth register to get:

$$\frac{1}{\sqrt{R}} \sum_{r=1}^R U_{\mathbf{v}_r^{\mathbf{X}^*}} |0\rangle_{23} |(\hat{\sigma}_r^{\mathbf{X}})^2\rangle_5 = \frac{1}{\sqrt{R}} \sum_{r=1}^R |\mathbf{v}_r^{\mathbf{X}^*}\rangle_{23} |(\hat{\sigma}_r^{\mathbf{X}})^2\rangle_5. \quad (\text{S.69})$$

(3) Uncompute the fifth register by the inverse quantum SVD:

$$\frac{1}{\sqrt{R}} \sum_{r=1}^R |\mathbf{v}_r^{\mathbf{X}^*}\rangle_{23} |0\rangle_5. \quad (\text{S.70})$$

Here, the inverse quantum SVD consists of the inverse quantum Fourier transform of the fifth register and the density matrix exponentiation multiplying  $\exp(-i\text{tr}_1(|\hat{\mathbf{X}}\rangle\langle\hat{\mathbf{X}}|)t)$  to the second and third register conditioned on the fifth register. The symbol  $\text{tr}_1$  signifies the partial trace with respect to the first register. Thus we can compute  $|\chi_2^{(0)}\rangle$  by  $R$  controlled- $U_{\mathbf{v}^*}$  operations and one inverse quantum SVD operation.

Lastly, we present the computation for  $|\chi_2\rangle$ : (1) Prepare the following state:

$$\sqrt{\frac{1}{1 + \frac{1}{4R}}} \left[ \frac{1}{\sqrt{R}} \sum_{r=1}^R |0\rangle_{23} |0\rangle_4 |(\hat{\sigma}_r^{\mathbf{X}})^2\rangle_5 + \frac{1}{2\sqrt{R|S_2^{(1)}|}} \sum_{r \in \text{ind } S_2^{(1)}} |0\rangle_{23} |1\rangle_4 |(\hat{\sigma}_r^{\mathbf{X}'})^2\rangle_5 \right], \quad (\text{S.71})$$

where

$$\text{ind } S_2^{(1)} := \left\{ r \in \{1, 2, \dots, R\} \mid |\mathbf{v}_r^{\mathbf{X}'^*}\rangle \in S_2^{(1)} \right\}. \quad (\text{S.72})$$

(2) Compute  $|\chi_2^{(0)}\rangle$  and  $|\phi_2^{(1)}\rangle$  conditionally on the fourth register in a similar way to the steps 2 and 3 of computing  $|\chi_2^{(0)}\rangle$  described above:

$$\sqrt{\frac{1}{1 + \frac{1}{4R}}} \left[ \frac{1}{\sqrt{R}} \sum_{r=1}^R |\mathbf{v}_r^{\mathbf{X}^*}\rangle_{23} |0\rangle_4 |0\rangle_5 + \frac{1}{2\sqrt{R|S_2^{(1)}|}} \sum_{r \in \text{ind } S_2^{(1)}} |\mathbf{v}_r^{\mathbf{X}'^*}\rangle_{23} |1\rangle_4 |0\rangle_5 \right]. \quad (\text{S.73})$$

(3) Apply the Hadamard gate to the fourth register. Then we have

$$\frac{1}{\sqrt{2}} \sqrt{\frac{1}{1 + \frac{1}{4R}}} \left[ \frac{1}{\sqrt{R}} \sum_{r=1}^R |\mathbf{v}_r^{\mathbf{X}^*}\rangle_{23} + \frac{1}{2\sqrt{R|S_2^{(1)}|}} \sum_{r \in \text{ind } S_2^{(1)}} |\mathbf{v}_r^{\mathbf{X}'^*}\rangle_{23} \right] |0\rangle_{45} + \dots \quad (\text{S.74})$$

(4) Measure the fourth and fifth registers. If the outcome corresponds to all zeros, we obtain  $|\chi_2\rangle_{23}|0\rangle_{45}$ . The success probability is  $1/(2 + 1/2R)$ , which is  $\Omega(1)$ . Therefore we can compute  $|\chi_2\rangle$  by  $O(R)$  controlled- $U_{\mathbf{v}^*}$  operations and  $O(1)$  inverse quantum SVD operations.

### C. Summary and concluding remarks

The example of the reference state preparation presented in this section demonstrates the existence of quantum circuits with polylogarithmic complexity in terms of  $N$ , capable of generating  $|\chi_1\rangle$  and  $|\chi_2\rangle$  such that  $1/\zeta = O(\text{poly } R)$ . The construction of these circuits necessitates the pure-state tomography of right singular vector states. Consequently, the computational complexity of constructing the presented circuits increases linearly with  $M$ , while the execution of the presented circuits is much more efficient with  $O(\text{poly log } M)$  complexity.

It is important to note that while this example serves as a theoretical construct to demonstrate that the qDMD algorithm can achieve an exponential speedup in  $N$ , it is not optimized for practical use. For specific problems, one may find more efficient ways to prepare reference states. For instance, methods like the automatic quantum circuit encoding [7] may construct quantum circuits that approximately generate singular vector states or their superpositions without exhaustive tomography. Furthermore, the value of  $\zeta$  may be enhanced in a variational manner in which a parameterized ansatz quantum circuit is tuned based on observed inner product values. Such variational method may improve the scaling of the computational complexity relative to  $R$ . The development of a pragmatic approach to the reference state preparation remains an open area for future research.

## III. COMPUTING DMD MODE STATES

### A. Recursive coherent state addition

The quantum circuit proposed by Oszmaniec et al. [8] (Fig. 5 of the main text) creates a coherent superposition of two quantum states  $|\psi_0\rangle$  and  $|\psi_1\rangle$ :

$$|\Psi\rangle = \alpha \frac{\langle\chi|\psi_1\rangle}{|\langle\chi|\psi_1\rangle|} |\psi_0\rangle + \beta \frac{\langle\chi|\psi_0\rangle}{|\langle\chi|\psi_0\rangle|} |\psi_1\rangle. \quad (\text{S.75})$$

Here,  $\alpha$  and  $\beta$  are user-specified complex amplitudes, and  $|\chi\rangle$  is a reference quantum state for the coherent addition. When  $|\psi_0\rangle$  and  $|\psi_1\rangle$  are orthogonal—the computation of DMD mode states satisfies this condition—the probability of successfully creating the coherent superposition is given by

$$\frac{|\langle\chi|\psi_0\rangle|^2 |\langle\chi|\psi_1\rangle|^2}{|\langle\chi|\psi_0\rangle|^2 + |\langle\chi|\psi_1\rangle|^2}. \quad (\text{S.76})$$

The created superposition can also be represented as

$$\begin{aligned} |\Psi\rangle &= \alpha e^{i\theta_1} |\psi_0\rangle + \beta e^{i\theta_0} |\psi_1\rangle \\ &= e^{i(\theta_0+\theta_1)} [\alpha e^{-i\theta_0} |\psi_0\rangle + \beta e^{-i\theta_1} |\psi_1\rangle], \end{aligned} \quad (\text{S.77})$$

where

$$\theta_i = \arg \langle\chi|\psi_i\rangle \quad (\text{S.78})$$

for  $i = 0, 1$ . If the global phase of  $|\psi_i\rangle$  is shifted by  $\theta$ , the phase  $\theta_i$  is also shifted by  $\theta$ . Therefore, the phase factor  $\exp(-i\theta_i)$  of the amplitude of  $|\psi_i\rangle$  ensures that the superposition state  $|\Psi\rangle$  is invariant up to its global phase under a global phase shift of  $|\psi_i\rangle$ . When  $\theta_0$  and  $\theta_1$  are known, including the phase factors  $\exp(i\theta_0)$  and  $\exp(i\theta_1)$  into user-specified amplitudes  $\alpha$  and  $\beta$ , one can create a superposition of two quantum states with arbitrary amplitudes.

One can also create a coherent superposition of multiple quantum states by recursively creating two-state coherent superpositions. This recursive coherent state addition process is illustrated in Fig. 1. In this figure, the multi-state coherent addition process proceeds from the bottom to the top; the superposition state at each branch node is created by the two-state coherent addition of its child nodes' states. One may adopt different reference states for each two-state coherent addition process to enhance the success probability of each process (see below).

A DMD mode state can be computed by the recursive coherent state addition protocol. Suppose we aim to compute a DMD mode state

$$|\tilde{w}_r\rangle \approx \sum_{r'=1}^R \tilde{w}_r^{r'} |\mathbf{u}_{r'}^{[\mathbf{X} \ \mathbf{X}']}\rangle. \quad (\text{S.79})$$

The recursive coherent state addition consists of  $R - 1$  steps of two-state coherent addition. A two-state coherent addition step indexed by  $k$  adds two quantum states

$$|\psi_{I_0^k}\rangle = \frac{1}{\sqrt{\sum_{r' \in I_0^k} |\tilde{w}_{r'}^{I_0^k}|^2}} \sum_{r' \in I_0^k} \tilde{w}_{r'}^{I_0^k} |\mathbf{u}_{r'}^{[\mathbf{X}, \mathbf{X}']}\rangle, \quad (\text{S.80})$$

$$|\psi_{I_1^k}\rangle = \frac{1}{\sqrt{\sum_{r' \in I_1^k} |\tilde{w}_{r'}^{I_1^k}|^2}} \sum_{r' \in I_1^k} \tilde{w}_{r'}^{I_1^k} |\mathbf{u}_{r'}^{[\mathbf{X}, \mathbf{X}']}\rangle, \quad (\text{S.81})$$

to create the superposition state

$$|\psi_{I_0^k \cup I_1^k}\rangle = \frac{1}{\sqrt{\sum_{r' \in I_0^k \cup I_1^k} |\tilde{w}_{r'}^{I_0^k \cup I_1^k}|^2}} \sum_{r' \in I_0^k \cup I_1^k} \tilde{w}_{r'}^{I_0^k \cup I_1^k} |\mathbf{u}_{r'}^{[\mathbf{X}, \mathbf{X}']}\rangle, \quad (\text{S.82})$$

where  $I_0^k$  and  $I_1^k$  are some mutually-exclusive sets of indices  $r'$ . Let  $|\chi_1\rangle$  be a reference state for estimating  $\tilde{\mathbf{K}}'$  and  $|\chi_{\text{add}}^k\rangle$  be a reference state for the two-state addition of step  $k$ . Using the three-state SWAP test for  $|\chi_1\rangle$ ,  $|\chi_{\text{add}}^k\rangle$ , and  $|\mathbf{u}_{r'}^{[\mathbf{X}, \mathbf{X}']}\rangle$ , we can estimate  $\langle \chi_1 | \chi_{\text{add}}^k \rangle \langle \chi_{\text{add}}^k | \mathbf{u}_{r'}^{[\mathbf{X}, \mathbf{X}']}\rangle \langle \mathbf{u}_{r'}^{[\mathbf{X}, \mathbf{X}']} | \chi_1 \rangle$ . Since  $\langle \mathbf{u}_{r'}^{[\mathbf{X}, \mathbf{X}']} | \chi_1 \rangle$  is known through the estimation of  $\tilde{\mathbf{K}}'$ , we can estimate  $\langle \chi_1 | \chi_{\text{add}}^k \rangle \langle \chi_{\text{add}}^k | \mathbf{u}_{r'}^{[\mathbf{X}, \mathbf{X}']}\rangle$ . Therefore, an estimate of  $\langle \chi_1 | \chi_{\text{add}}^k \rangle \langle \chi_{\text{add}}^k | \psi_{I_j^k} \rangle$  ( $j = 0, 1$ ) can be derived as

$$\langle \chi_1 | \chi_{\text{add}}^k \rangle \langle \chi_{\text{add}}^k | \psi_{I_j^k} \rangle = \frac{1}{\sqrt{\sum_{r' \in I_j^k} |\tilde{w}_{r'}^{I_j^k}|^2}} \sum_{r' \in I_j^k} \tilde{w}_{r'}^{I_j^k} \langle \chi_1 | \chi_{\text{add}}^k \rangle \langle \chi_{\text{add}}^k | \mathbf{u}_{r'}^{[\mathbf{X}, \mathbf{X}']}\rangle. \quad (\text{S.83})$$

Based on this estimation, the user-specified amplitude of  $|\psi_{I_j^k}\rangle$  in the two-state addition process is set to

$$\sqrt{\frac{\sum_{r' \in I_j^k} |\tilde{w}_{r'}^{I_j^k}|^2}{\sum_{r' \in I_0^k \cup I_1^k} |\tilde{w}_{r'}^{I_0^k \cup I_1^k}|^2}} e^{i\theta_{I_j^k}}, \quad (\text{S.84})$$

where

$$\begin{aligned} \theta_{I_j^k} &= \arg(\langle \chi_1 | \chi_{\text{add}}^k \rangle \langle \chi_{\text{add}}^k | \psi_{I_j^k} \rangle) \\ &= \arg \langle \chi_1 | \chi_{\text{add}}^k \rangle + \arg \langle \chi_{\text{add}}^k | \psi_{I_j^k} \rangle. \end{aligned} \quad (\text{S.85})$$

Note that  $\arg \langle \chi_1 | \chi_{\text{add}}^k \rangle$  in  $\theta_{I_0^k}$  and  $\theta_{I_1^k}$  only affects the global phase of the resulting superposition state.

## B. Computational complexity

Let us evaluate the computational complexity of computing a DMD mode state with keeping the phase error of each amplitude  $\tilde{w}_{r'}^{I_0^k}$  below  $\epsilon$ . The computational complexity consists of two contributing parts: (1) the computational

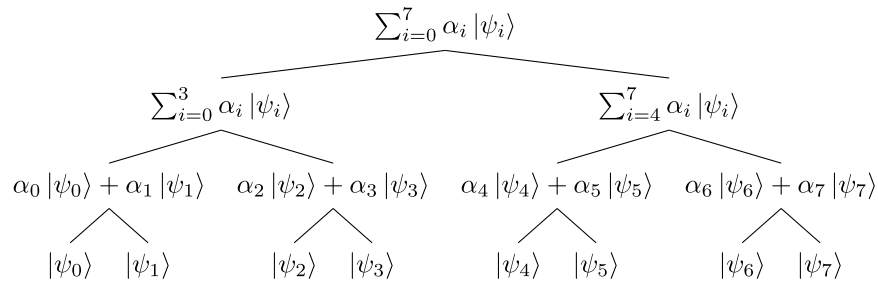


FIG. 1. Recursive coherent state addition for creating a superposition of multiple quantum states. This figure illustrates the case for an eight-state superposition. The root node represents the target superposition of multiple quantum states. The leaf nodes correspond to elementary quantum states comprising the target superposition. Each branch node (a non-leaf node) represents a coherent superposition of its child nodes, up to normalization. The process advances from the bottom to the top, where the superposition at each branch node is created from the coherent addition of its child nodes.

complexity of estimating phases  $\theta_{I_0^k}$  and  $\theta_{I_1^k}$  at all steps  $k$  and (2) the computational complexity of the recursive coherent state addition. In the following evaluation, we omit the computational costs for reference state preparations, which will be considered in the next subsection.

First, we consider the computational complexity of estimating phases  $\theta_{I_0^k}$  and  $\theta_{I_1^k}$  at all steps  $k$ . Because the tree depth for the recursive coherent state addition is  $\lceil \log_2 R \rceil$ , the tolerant phase error at each step is  $\epsilon / \lceil \log_2 R \rceil$ . Therefore, at each step  $k$ , it is necessary to estimate  $\langle \chi_1 | \chi_{\text{add}}^k \rangle \langle \chi_{\text{add}}^k | \psi_{I_j^k} \rangle$  with precision

$$|\langle \chi_1 | \chi_{\text{add}}^k \rangle \langle \chi_{\text{add}}^k | \psi_{I_j^k} \rangle| \frac{\epsilon}{\lceil \log_2 R \rceil} \quad (\text{S.86})$$

2. The upper bound of the error of  $\langle \chi_1 | \chi_{\text{add}}^k \rangle \langle \chi_{\text{add}}^k | \psi_{I_j^k} \rangle$  can be evaluated in terms of the maximum error among all terms of  $\langle \chi_1 | \chi_{\text{add}}^k \rangle \langle \chi_{\text{add}}^k | \psi_{I_j^k} \rangle$ , denoted by  $\epsilon_{\text{term}}$ , as

$$\frac{\sum_{r' \in I_j^k} |\tilde{w}_{r'}^{r'}|}{\sqrt{\sum_{r' \in I_j^k} |\tilde{w}_{r'}^{r'}|^2}} \epsilon_{\text{term}} \leq \sqrt{|I_j^k|} \epsilon_{\text{term}} \leq \sqrt{R} \epsilon_{\text{term}}. \quad (\text{S.87})$$

The first inequality follows the Cauchy–Schwarz inequality. Consequently,

$$\epsilon_{\text{term}} = |\langle \chi_1 | \chi_{\text{add}}^k \rangle \langle \chi_{\text{add}}^k | \psi_{I_j^k} \rangle| \frac{\epsilon}{\sqrt{R} \lceil \log_2 R \rceil} \quad (\text{S.88})$$

is a sufficient condition for the desired total precision. This precision  $\epsilon_{\text{term}}$  is achieved when the three-state SWAP test estimates  $\langle \chi_1 | \chi_{\text{add}}^k \rangle \langle \chi_{\text{add}}^k | \mathbf{u}_{r'}^{[\mathbf{X} \ \mathbf{X}']} \rangle \langle \mathbf{u}_{r'}^{[\mathbf{X} \ \mathbf{X}']} | \chi_1 \rangle$  with precision

$$|\langle \chi_1 | \chi_{\text{add}}^k \rangle \langle \chi_{\text{add}}^k | \psi_{I_j^k} \rangle \langle \mathbf{u}_{r'}^{[\mathbf{X} \ \mathbf{X}']} | \chi_1 \rangle| \frac{\epsilon}{\sqrt{R} \lceil \log_2 R \rceil}. \quad (\text{S.89})$$

Let us define parameters  $\zeta_3$  and  $\zeta_4$  as

$$\zeta_3 := \min_k |\langle \chi_1 | \chi_{\text{add}}^k \rangle|^2, \quad (\text{S.90})$$

$$\zeta_4 := \min_k \min_{j \in \{0,1\}} |\langle \chi_{\text{add}}^k | \psi_{I_j^k} \rangle|^2, \quad (\text{S.91})$$

where  $\min_k$  signifies the minimum over all step-indices  $k$ . Additionally,  $\zeta_1$  defined in Eq. (S.11) is a lower bound for  $|\langle \mathbf{u}_{r'}^{[\mathbf{X} \ \mathbf{X}']} | \chi_1 \rangle|^2$ . Using these parameters, we can express the required number of copies of each  $|\mathbf{u}_{r'}^{[\mathbf{X} \ \mathbf{X}']}\rangle$  for estimating the phase factors at each step as  $O(R(\log_2 R)^2 / \zeta_1 \zeta_3 \zeta_4 \epsilon^2)$ . Because each  $|\mathbf{u}_{r'}^{[\mathbf{X} \ \mathbf{X}']}\rangle$  is involved in  $\lceil \log_2 R \rceil$  steps of two-state coherent addition, the required number of quantum SVDs for estimating all phase factors is

$$O\left(\frac{\kappa_{[\mathbf{X} \ \mathbf{X}']}^2}{\zeta_1 \zeta_3 \zeta_4 \epsilon^2} R^2 (\log_2 R)^3 \log(\kappa_{[\mathbf{X} \ \mathbf{X}']}^2 \log R)\right), \quad (\text{S.92})$$

due to Eq. (S.9). The parameter  $\kappa_{[\mathbf{X} \ \mathbf{X}]}$  is the condition number of  $[\mathbf{X} \ \mathbf{X}']$  (see Eq. (S.8)). The gate complexity is larger than the required number of quantum SVDs by a factor of  $T/\epsilon^2 \text{ poly log}(NM/\epsilon)$ .

Next, we consider the computational complexity of the recursive coherent addition. The success probability at step  $k$  can be bounded from below as

$$\frac{|\langle \chi_{\text{add}}^k | \psi_{I_0^k} \rangle|^2 |\langle \chi_{\text{add}}^k | \psi_{I_1^k} \rangle|^2}{|\langle \chi_{\text{add}}^k | \psi_{I_0^k} \rangle|^2 + |\langle \chi_{\text{add}}^k | \psi_{I_1^k} \rangle|^2} \geq \frac{1}{2} \min\{|\langle \chi_{\text{add}}^k | \psi_{I_0^k} \rangle|^2, |\langle \chi_{\text{add}}^k | \psi_{I_1^k} \rangle|^2\} \geq \frac{\zeta_4}{2}. \quad (\text{S.93})$$

Therefore,  $O(2/\zeta_4)$  copies of  $|\psi_{I_j^k}\rangle$  ( $j = 0, 1$ ) are required for successfully creating a superposition state at step  $k$ . Because the tree depth for the recursive coherent state addition is  $\lceil \log_2 R \rceil < \log_2 R + 1$ , the required number of copies of  $|\mathbf{u}_{r'}^{[\mathbf{X} \ \mathbf{X}']}\rangle$  is  $O((2/\zeta_4)^{\log_2 R + 1})$  in total. Due to Eq. (S.9), the required number of quantum SVDs for the recursive coherent state addition is

$$O\left(\frac{\kappa_{[\mathbf{X} \ \mathbf{X}']}^2}{\zeta_4} R^{2 + \log_2 \frac{1}{\zeta_4}} \log(\kappa_{[\mathbf{X} \ \mathbf{X}']}^2 \log R)\right). \quad (\text{S.94})$$

The gate complexity is larger than the required number of quantum SVDs by a factor of  $T/\epsilon^2 \text{ poly log}(NM/\epsilon)$ .

<sup>2</sup> Let  $\tilde{z}$  be an estimate of a complex value  $z$  and  $\epsilon_z$  denote the estimation error, i.e.,  $\tilde{z} = z + \epsilon_z$ . On the complex plane,  $\epsilon_z$  can be viewed as a vector from the point  $z$  to the point  $\tilde{z}$ . When the vector  $\epsilon_z$  is perpendicular to the radial direction of  $z$ , the phase error  $\epsilon_{\text{phase}} = |\arg \tilde{z} - \arg z|$  takes the maximum value  $\arcsin(|\epsilon_z/z|)$ . Because  $\arcsin(|\epsilon_z/z|)$  is less than  $|\epsilon_z/z|$ , the estimation of  $z$  with precision  $|z|\epsilon$  ensures that the phase error is less than  $\epsilon$ .

### C. Reference state preparation

One may use any reference state at each step of the recursive coherent state addition provided that  $\zeta_3$  and  $\zeta_4$  are both positive. Regardless of the choice of reference states, superposition states to be computed are identical within a tolerant error. However, the choice of reference states affects the computational complexity; the larger  $\zeta_3$  and  $\zeta_4$  are, the shorter the computational time is.

A set of reference states with large  $\zeta_3$  and  $\zeta_4$  may be found by a variational quantum algorithm. Let  $U_k(\boldsymbol{\theta}_k)$  be an ansatz quantum circuit for generating a reference state of step  $k$ :  $U_k(\boldsymbol{\theta}_k)|0\rangle = |\chi_{\text{add}}^k(\boldsymbol{\theta}_k)\rangle$ . Here,  $\boldsymbol{\theta}_k$  denotes circuit parameters to be optimized. In this setup,  $\zeta_3$  and  $\zeta_4$  are considered as functions of  $\{\boldsymbol{\theta}_k\}$ . The optimal values of  $\{\boldsymbol{\theta}_k\}$  can be found by solving the following optimization problem:

$$\underset{\{\boldsymbol{\theta}_k\}}{\text{maximize}} \min\{\zeta_3(\{\boldsymbol{\theta}_k\}), \zeta_4(\{\boldsymbol{\theta}_k\})\}. \quad (\text{S.95})$$

Using a solution of the optimization problem, denoted by  $\{\boldsymbol{\theta}_k^*\}$ , the reference state of each step  $k$  is prepared by  $U_k(\boldsymbol{\theta}_k^*)$ .

We can also compute a set of reference states such that  $1/\zeta_3 = O(1)$  and  $1/\zeta_4 = O(1)$  with another protocol. These conditions on  $\zeta_3$  and  $\zeta_4$  imply that the required number of quantum SVDs for computing a DMD mode state is  $O(\text{poly } R)$ . In what follows, we present a specific procedure for reference state preparation satisfying these conditions.

Initially, we perform pure-state tomography [3] to estimate all right singular vector states of  $[\mathbf{X} \ \mathbf{X}']$ . The pure-state tomography requires an  $O(M)$  runtime for each right singular vector state. Subsequently, for each right singular vector state  $|\mathbf{v}_{r'}^{[\mathbf{X} \ \mathbf{X}']*}\rangle$ , we construct a quantum circuit  $V_{r'}$  such that  $V_{r'}|0\rangle = \exp(-i\varphi_{r'})|\mathbf{v}_{r'}^{[\mathbf{X} \ \mathbf{X}']*}\rangle$ . Here  $\varphi_{r'}$  signifies an unknown global phase which cannot be determined by the pure-state tomography. When the classical data of the amplitudes of  $|\mathbf{v}_{r'}^{[\mathbf{X} \ \mathbf{X}']*}\rangle$  is given, such a quantum circuit can be implemented with a gate complexity of  $O(\text{poly log } M)$  [4, 5].

Next, we show that a superposition state of the form

$$\sum_{r'=1}^R \alpha_{r'} e^{i\varphi_{r'}} |\mathbf{u}_{r'}^{[\mathbf{X} \ \mathbf{X}']}\rangle \quad (\text{S.96})$$

can be computed for arbitrary user-specified amplitudes  $\boldsymbol{\alpha} = [\alpha_1, \dots, \alpha_R]^\top$  such that  $\|\boldsymbol{\alpha}\| = 1$ , using the quantum SVD and controlled- $V_{r'}^\dagger$  operations. The computation is composed of the following steps: (1) Prepare  $|\text{SVD}([\mathbf{X} \ \widehat{\mathbf{X}}'])\rangle_{1:5}$ . (2) Uncompute the second to fourth registers by controlled- $V_{r'}^\dagger$  operations conditioned on the fifth register:

$$\begin{aligned} & \sum_{r'=1}^R \hat{\sigma}_{r'}^{[\mathbf{X} \ \mathbf{X}']} |\mathbf{u}_{r'}^{[\mathbf{X} \ \mathbf{X}']}\rangle_1 V_{r'}^\dagger |\mathbf{v}_{r'}^{[\mathbf{X} \ \mathbf{X}']*}\rangle_{234} |(\hat{\sigma}_{r'}^{[\mathbf{X} \ \mathbf{X}']})^2\rangle_5 \\ &= \sum_{r'=1}^R \hat{\sigma}_{r'}^{[\mathbf{X} \ \mathbf{X}']} e^{i\varphi_{r'}} |\mathbf{u}_{r'}^{[\mathbf{X} \ \mathbf{X}']}\rangle_1 |0\rangle_{234} |(\hat{\sigma}_{r'}^{[\mathbf{X} \ \mathbf{X}']})^2\rangle_5. \end{aligned} \quad (\text{S.97})$$

(3) Append an ancilla qubit as the sixth register. (4) Apply controlled rotations of the ancilla qubit conditioned on the fifth register to yield

$$\sum_{r'=1}^R \hat{\sigma}_{r'}^{[\mathbf{X} \ \mathbf{X}']} e^{i\varphi_{r'}} |\mathbf{u}_{r'}^{[\mathbf{X} \ \mathbf{X}']}\rangle_1 |0\rangle_{234} |(\hat{\sigma}_{r'}^{[\mathbf{X} \ \mathbf{X}']})^2\rangle_5 \left[ \frac{a\alpha_{r'}}{\hat{\sigma}_{r'}^{[\mathbf{X} \ \mathbf{X}']}} |0\rangle_6 + \sqrt{1 - \left| \frac{a\alpha_{r'}}{\hat{\sigma}_{r'}^{[\mathbf{X} \ \mathbf{X}']}} \right|^2} |1\rangle_6 \right], \quad (\text{S.98})$$

where

$$a = \min_{r'} \frac{\hat{\sigma}_{r'}^{[\mathbf{X} \ \mathbf{X}']}}{\alpha_{r'}}. \quad (\text{S.99})$$

(5) Uncompute the fifth register by the inverse operation of the quantum SVD. (6) Measure the second to sixth registers. If all measured values are zero, we obtain the target superposition state. The success probability is  $|a|^2$ , bounded from below as

$$|a|^2 \geq \min_{r'} (\hat{\sigma}_{r'}^{[\mathbf{X} \ \mathbf{X}']})^2 = \left( \frac{1}{\kappa_{[\mathbf{X} \ \mathbf{X}']}^2 R} \right). \quad (\text{S.100})$$

Here,  $\kappa_{[\mathbf{X} \ \mathbf{X}']}$  is the condition number of  $[\mathbf{X} \ \mathbf{X}']$  (see Eq. (S.8)), and we use Eq. (S.16) to derive the lower bound. Therefore, the required number of quantum SVDs for this computation is  $O(\kappa_{[\mathbf{X} \ \mathbf{X}']}^2 R)$ .

It is worth noting that the target superposition state created by the above protocol contains unknown phase factors  $\exp(i\varphi_{r'})$ ; thus the above protocol cannot be utilized for computing DMD mode states. However, this protocol is helpful for preparing reference states as described below. Hereinafter, we call the above protocol as *out-of-phase superposition protocol*.

The reference state  $|\chi_{\text{add}}^k\rangle$  of step  $k$  that we aim to compute using the out-of-phase superposition protocol is given by

$$|\chi_{\text{add}}^k\rangle = \frac{1}{\sqrt{2}} \left[ e^{i\varphi_0^k} |\psi_{I_0^k}\rangle + e^{i\varphi_1^k} |\psi_{I_1^k}\rangle \right], \quad (\text{S.101})$$

where  $\varphi_j^k$ 's signify arbitrary relative phases. The computability of the reference state  $|\chi_{\text{add}}^k\rangle$  follows the computability of  $\exp(i\varphi_j^k)|\psi_{I_j^k}\rangle$  ( $j = 0, 1$ ) due to the following reason: Suppose  $\exp(i\varphi_j^k)|\psi_{I_j^k}\rangle$  ( $j = 0, 1$ ) is computable using the out-of-phase superposition protocol. In other words, we supposed that a user-specified amplitude  $\alpha_j^k$  for computing  $\exp(i\varphi_j^k)|\psi_{I_j^k}\rangle$  is known. Let us define  $\alpha_{\text{add}}^k$  as

$$\alpha_{\text{add}}^k := \frac{\alpha_0^k + \alpha_1^k}{\sqrt{2}}. \quad (\text{S.102})$$

The out-of-phase superposition protocol with  $\alpha_{\text{add}}^k$  yields the reference state  $|\chi_{\text{add}}^k\rangle$  defined by Eq. (S.101). Now, we prove the computability of  $\exp(i\varphi_j^k)|\psi_{I_j^k}\rangle$  ( $j = 0, 1$ ) for all  $k$  by mathematical induction with respect to the recursion depth. (1) For any step  $k$  corresponding to one of the deepest branch nodes of the recursion tree (see Fig. 1),  $|\psi_{I_j^k}\rangle$  is a left singular vector state of  $[\mathbf{X} \ \mathbf{X}']$ , thus the statement holds. (2) For step  $k$  not corresponding to one of the deepest branch nodes, assume that the statement holds for all descendant steps of step  $k$ . Let  $k_c$  denote the index of a child step of step  $k$ . Due to the induction hypothesis, we can compute  $|\psi_{I_0^{k_c} \cup I_1^{k_c}}\rangle$  by recursively performing the descendant steps with the reference states defined in Eq. (S.101). Furthermore, we can compute

$$\begin{aligned} |\tilde{\psi}_{I_0^{k_c} \cup I_1^{k_c}}(\vartheta^{k_c})\rangle &= \frac{e^{i\varphi_0^{k_c}}}{\sqrt{\sum_{r' \in I_0^{k_c} \cup I_1^{k_c}} |\tilde{w}_{r'}^{k_c}|^2}} \sum_{r' \in I_0^{k_c}} \tilde{w}_{r'}^{k_c} |\mathbf{u}_{r'}^{[\mathbf{X} \ \mathbf{X}']}\rangle \\ &+ \frac{e^{i(\varphi_1^{k_c} + \vartheta^{k_c})}}{\sqrt{\sum_{r' \in I_0^{k_c} \cup I_1^{k_c}} |\tilde{w}_{r'}^{k_c}|^2}} \sum_{r' \in I_1^{k_c}} \tilde{w}_{r'}^{k_c} |\mathbf{u}_{r'}^{[\mathbf{X} \ \mathbf{X}']}\rangle \end{aligned} \quad (\text{S.103})$$

by the out-of-phase superposition protocol. Here,  $\vartheta^{k_c} \in [0, 2\pi)$  is a control parameter, and the user-specified amplitudes for computing the state is given by

$$\sqrt{\frac{\sum_{r' \in I_0^{k_c}} |\tilde{w}_{r'}^{k_c}|^2}{\sum_{r' \in I_0^{k_c} \cup I_1^{k_c}} |\tilde{w}_{r'}^{k_c}|^2}} \alpha_0^{k_c} + e^{i\vartheta^{k_c}} \sqrt{\frac{\sum_{r' \in I_1^{k_c}} |\tilde{w}_{r'}^{k_c}|^2}{\sum_{r' \in I_0^{k_c} \cup I_1^{k_c}} |\tilde{w}_{r'}^{k_c}|^2}} \alpha_1^{k_c}. \quad (\text{S.104})$$

The fidelity  $|\langle \tilde{\psi}_{I_0^{k_c} \cup I_1^{k_c}}(\vartheta^{k_c}) | \psi_{I_0^{k_c} \cup I_1^{k_c}} \rangle|^2$  takes a maximum value of one if and only if  $\vartheta^{k_c} = \varphi_0^{k_c} - \varphi_1^{k_c}$ . The parameter  $\vartheta^{k_c*}$  maximizing the fidelity can be found through a grid search based on the fidelity measurement. The quantum state  $|\tilde{\psi}_{I_0^{k_c} \cup I_1^{k_c}}(\vartheta^{k_c*})\rangle$  is equivalent to  $|\psi_{I_0^{k_c} \cup I_1^{k_c}}\rangle$  ( $= |\psi_{I_j^k}\rangle$ ) up to a global phase. Thus the statement holds for step  $k$ .

The reference states defined in Eq. (S.101) satisfy

$$|\langle \chi_{\text{add}}^k | \psi_{I_j^k} \rangle|^2 = \frac{1}{2} \quad (\text{S.105})$$

for all  $k$  and  $j$ ; thus  $1/\zeta_4 = 2$ . In contrast,  $|\langle \chi_1 | \chi_{\text{add}}^k \rangle|$  could be close to zero for some  $k$ , leading to a situation where  $1/\zeta_3$  becomes excessively large. This problem can be resolved by the following modification: Let  $b$  be a positive constant less than  $1/\sqrt{2}$ . When the reference state satisfies  $|\langle \chi_1 | \chi_{\text{add}}^k \rangle| \leq b/2$ , we modify the reference state to  $|\chi_{\text{add}'}^k\rangle$ :

$$|\chi_{\text{add}'}^k\rangle = \mathcal{C}_{\text{add}'}^k [|\chi_{\text{add}}^k\rangle + b|\chi_1\rangle], \quad (\text{S.106})$$

where  $\mathcal{C}_{\text{add}'}^k$  denotes the normalizing constant. The normalizing constant is bounded from below as

$$\begin{aligned} \mathcal{C}_{\text{add}'}^k &= \frac{1}{\| |\chi_{\text{add}'}^k \rangle + b |\chi_1 \rangle \|} \\ &\geq \frac{1}{\| |\chi_{\text{add}'}^k \rangle \| + b \| |\chi_1 \rangle \|} = \frac{1}{1+b} \end{aligned} \quad (\text{S.107})$$

Therefore, the modified reference state satisfies

$$\begin{aligned} |\langle \chi_1 | \chi_{\text{add}'}^k \rangle| &\geq \mathcal{C}_{\text{add}'}^k [b |\langle \chi_1 | \chi_1 \rangle| - |\langle \chi_1 | \chi_{\text{add}'}^k \rangle|] \\ &\geq \frac{1}{1+b} \left( b - \frac{b}{2} \right) = \frac{b}{2(1+b)} \end{aligned} \quad (\text{S.108})$$

and

$$\begin{aligned} |\langle \chi_{\text{add}'}^k | \psi_{I_j^k} \rangle| &\geq \mathcal{C}_{\text{add}'}^k \left[ |\langle \chi_{\text{add}'}^k | \psi_{I_j^k} \rangle| - b |\langle \chi_1 | \psi_{I_j^k} \rangle| \right] \\ &\geq \frac{1}{1+b} \left( \frac{1}{\sqrt{2}} - b \right) > 0. \end{aligned} \quad (\text{S.109})$$

Consequently,  $1/\zeta_3 = O(1)$  and  $1/\zeta_4 = O(1)$ . Since the required number of quantum SVDs for the out-of-phase superposition protocol scales as  $O(R)$  with respect to  $R$ , the overall number of quantum SVDs necessary for computing a DMD mode state is  $O(\text{poly } R)$ . The gate complexity is larger than the required number of quantum SVDs by a factor of  $T/\epsilon^2 \text{poly } \log(NM/\epsilon)$ .

#### IV. DYNAMIC MODE DECOMPOSITION FOR DEFECTIVE SYSTEMS

The qDMD algorithm presented in the main text assumes that the matrix  $\mathbf{A}$  is diagonalizable. This assumption implies that  $\mathbf{K}$  is also diagonalizable, thus its projected approximation  $\tilde{\mathbf{K}}'$  is assumed to have the eigenvalue decomposition. In this section, we consider a situation where  $\mathbf{A}$  is not diagonalizable. Such a non-diagonalizable matrix is said to be *defective* [9].

Any square matrix  $\mathbf{A} \in \mathbb{C}^{N \times N}$  can be expressed in the Jordan normal form [9] as

$$\mathbf{A} = \mathbf{P} \begin{pmatrix} \mathbf{J}_1 & & \\ & \ddots & \\ & & \mathbf{J}_p \end{pmatrix} \mathbf{P}^{-1}, \quad (\text{S.110})$$

where  $\mathbf{P}$  is an  $N \times N$  invertible matrix,  $\mathbf{J}_k$  ( $k = 1, \dots, p$ ) denotes a Jordan block. The  $k$ -th Jordan block is defined by

$$\mathbf{J}_k = \begin{pmatrix} \lambda_k^{\mathbf{A}} & 1 & & \\ & \lambda_k^{\mathbf{A}} & \ddots & \\ & & \ddots & 1 \\ & & & \lambda_k^{\mathbf{A}} \end{pmatrix} \in \mathbb{C}^{m_k \times m_k}, \quad (\text{S.111})$$

where  $\lambda_k^{\mathbf{A}}$  is an eigenvalue of  $\mathbf{A}$ , and  $m_k$  is the order of the Jordan block. The block diagonal matrix  $\text{diag}(\mathbf{J}_1, \dots, \mathbf{J}_p)$  is called as the Jordan normal form of  $\mathbf{A}$ . If  $m_k = 1$  for all  $k \in \{1, \dots, p\}$ , the Jordan normal form is a diagonal matrix, thus  $\mathbf{A}$  is diagonalizable; otherwise,  $\mathbf{A}$  is defective. Using the Jordan normal form, we can calculate the time-evolution operator  $\mathbf{K}$  as

$$\begin{aligned} \mathbf{K} &= \exp(\Delta t \mathbf{A}) \\ &= \mathbf{P} \begin{pmatrix} \exp(\Delta t \mathbf{J}_1) & & \\ & \ddots & \\ & & \exp(\Delta t \mathbf{J}_p) \end{pmatrix} \mathbf{P}^{-1}. \end{aligned} \quad (\text{S.112})$$

The exponential of a Jordan block is given by

$$\exp(\Delta t \mathbf{J}_k) = e^{\Delta t \lambda_k^{\mathbf{A}}} \begin{pmatrix} 1 & \frac{\Delta t}{1!} & \dots & \frac{(\Delta t)^{m_k-1}}{(m_k-1)!} \\ & 1 & \ddots & \vdots \\ & & \ddots & \frac{\Delta t}{1!} \\ & & & 1 \end{pmatrix} \in \mathbb{C}^{m_k \times m_k}. \quad (\text{S.113})$$

For  $\Delta t \neq 0$ , this exponential  $\exp(\Delta t \mathbf{J}_k)$  has only one eigenvalue  $\exp(\Delta t \lambda_k^{\mathbf{A}})$  with geometric multiplicity  $m_k$ . Therefore, the Jordan normal form of  $\mathbf{K}$  is the same as that of  $\mathbf{A}$  except that each eigenvalue  $\lambda_k^{\mathbf{A}}$  is replaced by  $\exp(\Delta t \lambda_k^{\mathbf{A}})$ .

The qDMD algorithm, as well as the classical exact DMD algorithm [10], can estimate the time-evolution operator  $\mathbf{K}$  through  $\tilde{\mathbf{K}}'$  even for a defective system. This is because  $\tilde{\mathbf{K}}'$  is defined through the singular value decompositions of data matrices, where no assumption is made on the diagonalizability. However, for a defective system,  $\tilde{\mathbf{K}}'$  is (nearly) defective<sup>3</sup>, thus the eigenvalue decomposition of  $\tilde{\mathbf{K}}'$  is infeasible. The Schur-based DMD algorithm proposed by Thitsa et al. [11] is a numerically-stable DMD algorithm for such a (nearly) defective system. The Schur-based DMD algorithm computes the Schur decomposition of  $\tilde{\mathbf{K}}'$ , instead of its eigenvalue decomposition. The Schur decomposition of  $\tilde{\mathbf{K}}'$  is given by

$$\tilde{\mathbf{K}}' = \tilde{\mathbf{W}}'_{\text{Schur}} \tilde{\mathbf{S}}' \tilde{\mathbf{W}}'^{\dagger}_{\text{Schur}}, \quad (\text{S.114})$$

where  $\tilde{\mathbf{S}}'$  is an upper triangular matrix, and  $\tilde{\mathbf{W}}'_{\text{Schur}}$  is a unitary matrix. This decomposition provides an approximation of the Schur decomposition of  $\tilde{\mathbf{K}}$ ,

$$\tilde{\mathbf{K}} = \tilde{\mathbf{W}}_{\text{Schur}} \tilde{\mathbf{S}} \tilde{\mathbf{W}}^{\dagger}_{\text{Schur}}, \quad (\text{S.115})$$

as

$$\tilde{\mathbf{S}} \approx \tilde{\mathbf{S}}', \quad (\text{S.116})$$

$$\tilde{\mathbf{W}}_{\text{Schur}} \approx \mathbf{Q} \tilde{\mathbf{W}}'_{\text{Schur}}. \quad (\text{S.117})$$

Here,  $\mathbf{Q}$  is an  $N \times R$  matrix whose columns are the  $R$  dominant left singular vectors of  $[\mathbf{X} \ \mathbf{X}']$ . The column vectors of the transformation matrix  $\tilde{\mathbf{W}}_{\text{Schur}}$  can be computed in the same manner as step 5 of the qDMD algorithm presented in the main text. Therefore, the quantum procedures (steps 1–3 and 5) of the qDMD algorithm can be directly adapted to the quantum version of the Schur-based DMD algorithm for nearly defective systems.

- 
- [1] R. K. Brayton, On the asymptotic behavior of the number of trials necessary to complete a set with random selection, *Journal of Mathematical Analysis and Applications* **7**, 31 (1963).
  - [2] S. Kimmel, C. Y.-Y. Lin, G. H. Low, M. Ozols, and T. J. Yoder, Hamiltonian simulation with optimal sample complexity, *npj Quantum Information* **3**, 13 (2017).
  - [3] F. Verdeil and Y. Deville, Pure-state tomography with parallel unentangled measurements, *Physical Review A* **107**, 012408 (2023).
  - [4] I. Kerenidis and A. Prakash, Quantum recommendation systems, in *8th Innovations in Theoretical Computer Science Conference (ITCS 2017)*, Leibniz International Proceedings in Informatics (LIPIcs), Vol. 67 (Schloss Dagstuhl–Leibniz-Zentrum fuer Informatik, 2017) p. 49.
  - [5] K. Mitarai, M. Kitagawa, and K. Fujii, Quantum analog-digital conversion, *Physical Review A* **99**, 012301 (2019).
  - [6] M. Schuld, I. Sinayskiy, and F. Petruccione, Prediction by linear regression on a quantum computer, *Physical Review A* **94**, 022342 (2016).
  - [7] T. Shirakawa, H. Ueda, and S. Yunoki, Automatic quantum circuit encoding of a given arbitrary quantum state (2021), arXiv:2112.14524 [quant-ph].
  - [8] M. Oszmaniec, A. Grudka, M. Horodecki, and A. Wójcik, Creating a superposition of unknown quantum states, *Physical Review Letters* **116**, 110403 (2016).

---

<sup>3</sup> The Jordan normal form of  $\mathbf{K}$  may be structurally instable; small perturbations due to finite computational precision and estimation errors may make  $\tilde{\mathbf{K}}$  not strictly defective. In general, it is impossible to determine whether a matrix is defective or not in the presence of computational errors [9].



- [9] G. H. Golub and J. H. Wilkinson, Ill-conditioned eigensystems and the computation of the jordan canonical form, *SIAM review* **18**, 578 (1976).
- [10] J. H. Tu, C. W. Rowley, D. Luchtenburg, S. L. Brunton, and J. N. Kutz, On dynamic mode decomposition: Theory and applications, *Journal of Computational Dynamics* **1**, 391 (2014).
- [11] M. Thitsa, M. Cloutre, E. Verriest, S. Coogan, and C. Martin, A numerically stable dynamic mode decomposition algorithm for nearly defective systems, *IEEE Control Systems Letters* **5**, 67 (2020).